

PAH destruction and survival in the disks of T Tauri stars

R. Siebenmorgen¹ and E. Krügel²

¹ European Southern Observatory, Karl-Schwarzschildstr. 2, D-85748 Garching b. München, Germany

² Max-Planck-Institut für Radioastronomie, Auf dem Hügel 69, Postfach 2024, D-53010 Bonn, Germany

Received Month XX, 2009 / Accepted Month XX, 20XX

ABSTRACT

In Spitzer observations of Tauri stars and their disks, PAH features are detected in less than 10% of the objects, although the stellar photosphere is sufficiently hot to excite PAHs. To explain the deficiency, we discuss PAH destruction by photons assuming that the star has beside its photospheric emission also a FUV, an EUV and an X-ray component with fractional luminosity of 1%, 0.1% and 0.025%, respectively. As PAH destruction process we consider unimolecular dissociation and present a simplified scheme to estimate the location from the star where the molecules become photo-stable. We find that soft photons with energies below ~ 20 eV dissociate PAHs only up to short distances from the star ($r < 1$ AU); whereas dissociation by hard photons (EUV and X-ray) is so efficient that it would destroy all PAHs (from regions in the disk where they could be excited). As a possible path for PAH survival we suggest turbulent motions in the disk. They can replenish PAHs or remove them from the reach of hard photons. For standard disk models, where the surface density changes like r^{-1} and the mid plane temperature like $r^{-0.5}$, the critical vertical velocity for PAH survival is proportional to $r^{-3/4}$ and equals ~ 5 m/s at 10 AU which is in the range of expected velocities in the surface layer. The uncertainty in the parameters is large enough to explain both detection and non-detection of PAHs. Our approximate treatment also takes into account the presence of gas which, at the top of the disk, is ionized and at lower levels neutral.

Key words. dust, extinction – planetary systems: protoplanetary disks – infrared: stars – X-rays: stars – X-rays: ISM

1. Introduction

Infrared emission bands of PAHs can be used as a probe of the UV environment. They are commonly seen in the ISM, but also in young stellar objects such as Herbig Ae/Be stars (Waelkens et al. 1996, Siebenmorgen et al. 2000, Meeus et al. 2001, Peeters et al. 2002, van Boekel et al. 2004). The observed emission can be explained in models of an irradiated disk (Habart et al. 2004, Visser et al., 2007, Dullemond et al. 2007a).

ISO also looked at a few of the much fainter T Tauri stars but without a clear PAH detection (Siebenmorgen et al. 2000). In the Evans et al. (2003) legacy program which employs the more sensitive

Send offprint requests to: rsiebenm@eso.org

Spitzer Space Telescope (SST), 3 out of 38 T Tauri stars show PAH features (Geers et al. 2006). This corresponds to a detection rate of only 8% in contrast to almost 60% in Herbig Ae/Be stars (Acke & van den Ancker 2004). Similarly low rates for T Tauri stars are found by Furlan et al. (2006) who present 111 SST spectra in the Taurus-Auriga star forming region and speculate that the absence of PAH resonances is due to the much weaker UV field compared to Herbig Ae/Be stars. Geers et al. (2009), on the other hand, argue that the PAHs are simply under-abundant relative to the ISM. They also find that variations of the disk geometry, such as flaring or gaps, have only a small effect on the strength of the PAH bands. Clearing out gas and dust by planet formation inside the disk could effectively remove PAHs. Indeed, inner gaps in disks are observed at radii between 40–60 AU and at wavelengths between 20–1000 μm where the emission is dominated by large grains (Brown et al. 2008, Geers et al. 2007b). However, in cases where PAH emission is resolved, it is extended up to 15–60 AU, without sub-structure and inside the inner gap region (Geers et al. 2007a). The spatial extent of the PAH emission is also similar for T Tauri and Herbig Ae/Be stars. We therefore suggest that PAH removal by radiative destruction is dominant.

Present radiative transfer models of the PAH emission from dusty disks consider only the stellar radiation field and no additional EUV or X-ray component (Habart et al. 2004, Geers et al. 2006, Visser et al. 2007, Dullemond et al. 2007). Their hard photons could, according to laboratory experiments (Ruhl et al. 1989, Leach et al. 1989a,b, Jochims et al. 1994) and theory (Omont 1986, Tielens 2005, Rapacioli et al. 2006, Micelotta et al. 2009), destroy PAHs. We discuss below their impact on the PAH abundance in the disks of T Tauri stars.

2. Radiation components of T Tauri stars

Our T Tauri model star has a total luminosity $L_* = 2L_\odot$. Its radiation consists of a photospheric, a FUV, an EUV and an X-ray component. Their parameters are listed in Table 1 and are very similar to those proposed by Gorti & Hollenbach (2008). The total spectrum is displayed in Fig.1. We point out that the FUV and EUV radiation are observationally poorly constrained.

The photosphere supplies most of the luminosity whereas the FUV, EUV and X-ray radiation are much weaker and believed to originate from accretion onto the star and from chromospheric and coronal activity. The photosphere, the FUV and EUV component are approximated by blackbodies. We assume 4000 K for the photosphere and, following Stahler et al. (1980) and Calvet & Gullbring (1998), 15000 K for the FUV (pre-shock) and $\sim 3 \times 10^5$ K for the EUV emission (post-shock region).

The strength of the FUV and EUV radiation is determined by the accretion luminosity which we approximate by $L_{\text{acc}} = GM_*\dot{M}/R_*$. If $R_* = 2R_\odot$ and $M_* = 1M_\odot$ are the radius and mass of the star, an accretion rate $\dot{M} = 10^{-9} M_\odot \text{ yr}^{-1}$ (Akeson et al. 2005) yields $L_{\text{acc}} \sim 0.01 L_*$. Higher values ($L_{\text{acc}}/L_* \gtrsim 0.1$), but with a large spread, are derived by Muzerolle et al. (1998, 2003) from hydrogen emission lines. However, as we show in section 5, such stronger fluxes have little influence on the stability analysis of PAHs.

Preibisch et al. (2006) establish from Chandra observations (0.5–8 keV) a relation between the X-ray luminosity, L_x , and the total luminosity L_* confirming the ROSAT results of Sterzik & Schmitt (1997). The ratio L_x/L_* is similar in rapidly rotating main-sequence stars and non-accreting T Tauri stars ($\sim 10^{-3}$), but systematically lower by a factor ~ 4 in accreting T Tauri stars (Preibisch et al. 2006).

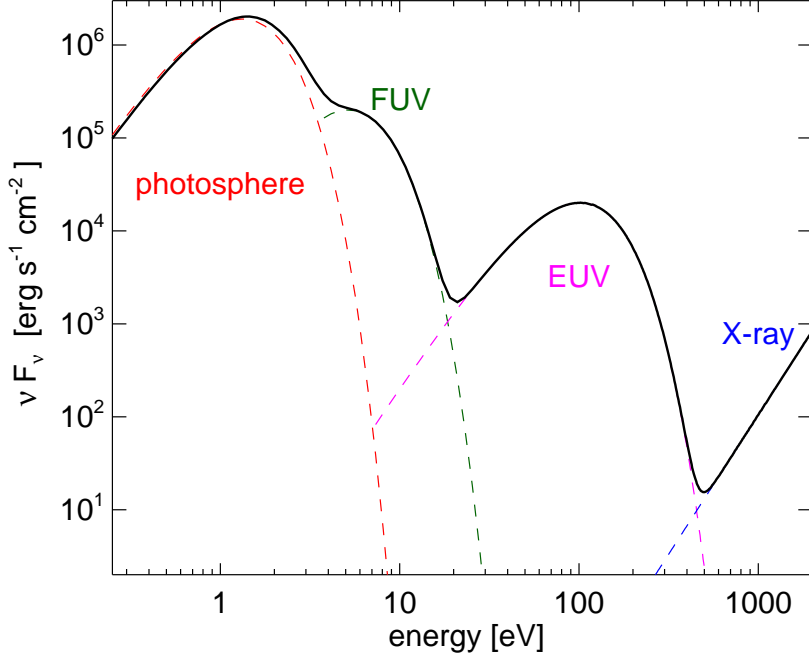


Fig. 1. The spectral energy distribution of our T Tauri model star at 1 AU without foreground extinction (Eq. 1). The absolute luminosities of the components are given in Table 1.

Table 1. The four radiation components of our T Tauri model star.

		(1)	(2)	(3)	(4)
i	component	L/L_*	spectrum	$h\bar{\nu}_{\text{em}}$ (eV)	F_{10} ($\text{erg s}^{-1}\text{cm}^{-2}$)
1	photosphere	0.99	4000 K BB	0.9	30 000
2	FUV	0.01	15000 K BB	3.5	300
3	EUV	0.001	3×10^5 K BB	70	30
4	X-rays ($h\nu < 2$ keV)	2.5×10^{-4}	$\propto \nu^2$	1330	10

- (1) fractional luminosity,
(2) spectral shape (BB = blackbody),
(3) mean energy of emitted photons, $h\bar{\nu}_{\text{em}}$,
(4) approximate flux at 10 AU, F_{10} .

Interestingly, in Herbig Ae/Be stars L_x/L_* is much smaller ($\sim 10^{-7} \dots 10^{-5}$, Stelzer et al. 2006) with values comparable to the Sun. The solar X-ray luminosity in the 0.1–2.4 keV ROSAT passband lies during a solar cycle in the range $10^{-6.8} \lesssim L_x/L_* \lesssim 10^{-5.7}$ and is typical for G stars (Judge et al. 2003).

X-ray fluxes are generally variable on timescales of hours to weeks and weaken during the evolution of the T Tauri star. For example, half of the sources in the Taurus molecular cloud detected by XMM/Newton (0.3 – 7.8 keV) show variations, more at hard (> 0.5 keV) than at soft energies, and a quarter of them

display flares (Stelzer et al. 2007), about once a week and lasting for a few hours. In a strong flare, more than 10^{35} erg are emitted and L_x can reach 1% of the total luminosity. We assume up to 2 keV a power law spectrum $\propto \nu^2$ (Güdel et al. 2007) and neglect harder radiation because the emission then steeply declines ($\propto \nu^{-3}$).

Let L_i be the frequency-integrated luminosity of the radiation component i (see Table 1) and $L_{i,\nu}$ its spectral luminosity such that $L_i = \int L_{i,\nu} d\nu$. Dropping for convenience the index i , the flux (of component i) at a distance r is

$$F_\nu = \frac{L_\nu e^{-\tau_\nu}}{4\pi r^2} \quad (1)$$

where we included a screening factor $e^{-\tau_\nu}$ to account for foreground absorption (by dust and gas). If κ_ν denotes the absorption cross section per carbon atom, a PAH of N_c carbon atoms absorbs in one second (from component i)

$$N_\gamma = N_c \int \frac{F_\nu \kappa_\nu}{h\nu} d\nu \quad (2)$$

photons of total energy

$$E_{\text{abs}} = N_c \int F_\nu \kappa_\nu d\nu \quad (3)$$

The inverse of N_γ is the average time between two absorption events,

$$t_{\text{abs}} = N_\gamma^{-1} \quad (4)$$

The mean photon energy equals

$$h\bar{\nu} = \frac{\int F_\nu \kappa_\nu d\nu}{\int \frac{F_\nu \kappa_\nu}{h\nu} d\nu} \quad (5)$$

3. Cross sections

As the light from the star enters the disk, it is attenuated by gas and dust. The absorption cross section of gas depends on the ionization stage of the atoms which is determined by the balance between recombination and photo-ionization. By far the most important atoms are, of course, hydrogen and helium with ionization potentials of 13.6 eV and 24.6 eV, respectively. Because the recombination rate is proportional to the square of the gas density which is high in the disk (section 5), the gas is ionized only in a thin surface layer ($A_V < 0.001$ mag, section 2.6 of Gorti & Hollenbach 2008). We use atomic cross sections of Morrison & McCommon (1982) and Balucinska-Church & McCommon (1992) and solar element abundances.

The dust cross sections are taken from the model of Krügel (2006) which describes standard dust. For X-rays, the absorption efficiency calculated from Mie theory must be corrected downwards. Hard photons can eject electrons from the grain and as these carry away kinetic energy, only part of the photon energy is deposited in the dust particle. The threshold, E_t , above which such a correction is necessary depends on the grain size; details are given in Dwek & Smith (1996). For a 10 \AA graphite particle, $E_t \sim 100 \text{ eV}$ and the reduction factor is roughly proportional to ν^{-1} .

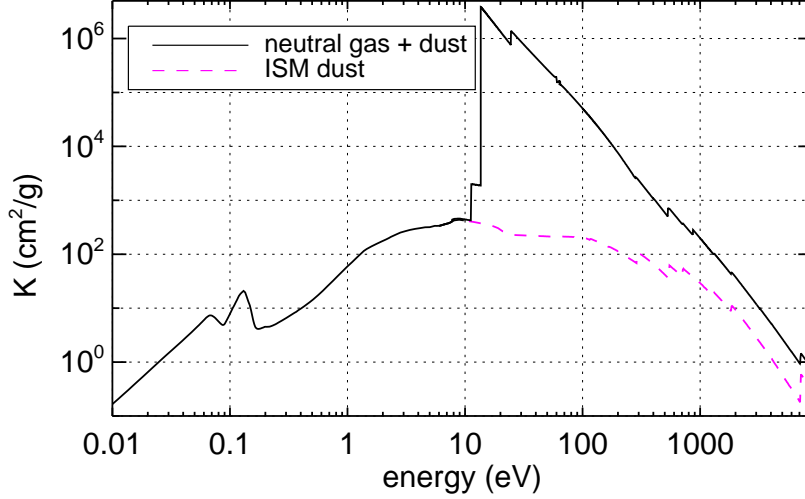


Fig. 2. The mass extinction coefficient per gram disk material when the gas is neutral (Morrison & McCommon 1983); the gas-to-dust mass ratio equals 130.

The absorption coefficient of dust, $K_{d,\lambda}$, and of neutral gas plus dust, $K_\lambda = K_{\text{gas},\lambda} + K_{d,\lambda}$, both per gram of disk material, are plotted in Fig. 2 for a dust-to-gas mass ratio of 1:130. Note that at the ionization threshold of hydrogen, K_{gas} is almost 10^4 times greater than K_d .

With respect to the absorption cross section of PAHs, we assume $\kappa_\nu = 7 \times 10^{-18} \text{ cm}^2$ per carbon atom when $h\nu < 13.6 \text{ eV}$ and scale κ_ν at higher energies to follow the values of a graphite sphere of 10 \AA radius (Dwek & Smith 1996). The maximum wavelength (in \AA) for PAH excitation is $\lambda_{\text{max,PAH}} = 1630 + 370\sqrt{N_c}$ (Schutte et al. 1993) resulting in a minimum photon energy of 2.3 eV for a PAH with $N_c = 100$ carbon atoms.

3.1. PAH emission

As the PAHs are transiently heated, their excitation is usually treated statistically. Following Guhathakurta & Draine (1989), let $P(T) dT$ be the probability of finding in a large ensemble of PAHs in a steady state an arbitrary PAH in the temperature interval $[T, T + dT]$. The temperature distribution function $P(T)$ is calculated in this method from a transition matrix (A_{fi}). If K_ν denotes the PAH absorption cross section, the matrix element A_{fi} referring to dust heating from an initial enthalpy bin centered at U_i to a final one centered at U_f and of width ΔU_f is, for a mono-chromatic flux, equal to

$$A_{fi} = \begin{cases} \frac{K_\nu F}{h\nu} & : \text{ if } |U_f - U_i - h\nu| \leq \frac{1}{2}\Delta U_f \\ 0 & : \text{ else} \end{cases} \quad (6)$$

Examples of $P(T)$ are displayed in Fig. 3 for mono-chromatic fluxes which cover almost the entire range encountered anywhere in the disk in terms of intensity, the flux ranges from $F = 10$ to $10^7 \text{ erg s}^{-1} \text{ cm}^{-2}$, as well as hardness, the photon energy is between $h\nu = 3.8 \text{ eV}$ and 1 keV . The approximate unattenuated fluxes of the four radiation components at a distance of 10 AU are listed in Table 1.

Note that when $F = n_\gamma h\nu$ is constant, the number of photons n_γ decreases as the photon energy $h\nu$ goes up. The power absorbed by one PAH is almost independent of the photon energy as long as $h\nu \lesssim 100$ eV (see Fig. 4). By and large, when $h\nu$ is fixed and F increases, the curves in Fig. 3 narrow and move to the right towards higher temperatures. When the radiation field is weak ($F = 10 \text{ erg s}^{-1} \text{ cm}^{-2}$) and the photons are soft ($h\nu = 3.8$ eV), the PAH absorbs about one photon per day and there is plenty of time to cool down. In this case, the PAH virtually never exceeds the sublimation temperature T_s , (at which solid carbon gasify). For a wide pressure range ($10^{-1} - 10^{-7} \text{ dyn cm}^{-2}$), $T_s \sim 2000$ K for graphite (CRC Handbook of Chemistry & Physics 2005, Salpeter et al. 1977). In Fig. 3 we highlight the area where the temperature is above T_s . For a PAH exposed to a strong radiation field ($F = 10^7 \text{ erg s}^{-1} \text{ cm}^{-2}$), about a dozen of soft photons are absorbed within a cooling time and the temperature distribution function becomes very narrow around 2000 K and sublimation is likely. For hard photons ($h\nu \geq 50$ eV), the PAH undergoes, independent of the strength of the radiation field, extreme temperature excursions. This indicates that PAH become photo-unstable either by absorption of a single hard photon, or by soft photons if there are many of them.

4. PAH destruction

The abundance of PAHs is determined by the competition between formation and destruction processes under the specific environmental conditions. Underlying processes are discussed, for example, by Omont (1986), Voit (1992), or recently by Micelotta et al. (2009a). Here we only consider PAH destruction by photons and generally assume that PAH formation is negligible. After photon absorption, a highly vibrationally excited PAH may relax through emission of IR photons or, if sufficiently excited, lose atoms. The latter process is called unimolecular dissociation and is discussed for interstellar PAHs by Allamandola (1989), Leger et al. (1989), Le Page et al. (2003), Rapacioli et al. (2006), and Micelotta et al. (2009b). Laboratory studies of PAH dissociation which can be applied to astrophysical situations are rare (Jochims et al. 1994). The photo-chemistry of PAHs is reviewed by Tielens (2005, 2008).

4.1. Procedure

In the disks of T Tau stars, the PAH abundance depends obviously on place and on time as the disk evolves. There is no general solution to the problem and to extract numbers, we have to radically simplify it. We wish to find some estimate of the location where PAHs become stable against photo-destruction. To derive a procedure, we recall that although after absorption of an energetic photon its energy is immediately distributed over all available vibrational modes (Allamandola et al., 1989), the excitation of a particular atom fluctuates and occasionally it is pushed into the continuum and leaves the PAH. Quantitatively, the unimolecular dissociation can be written in Arrhenius form. In a classical description, an atom of critical (Arrhenius) energy E_0 detaches from a PAH of peak temperature T_p if the dissociation time

$$t_{\text{dis}} \sim \nu_0^{-1} e^{E_0/kT_p} \quad (7)$$

is shorter than the cooling time t_{cool} . A characteristic value for the vibrational frequency is $\nu_0 \sim 10^{13} \text{ s}^{-1}$. The ‘‘atom’’, which may besides H or C also be an atomic group like C_2H_2 , needs the time t_{dis}

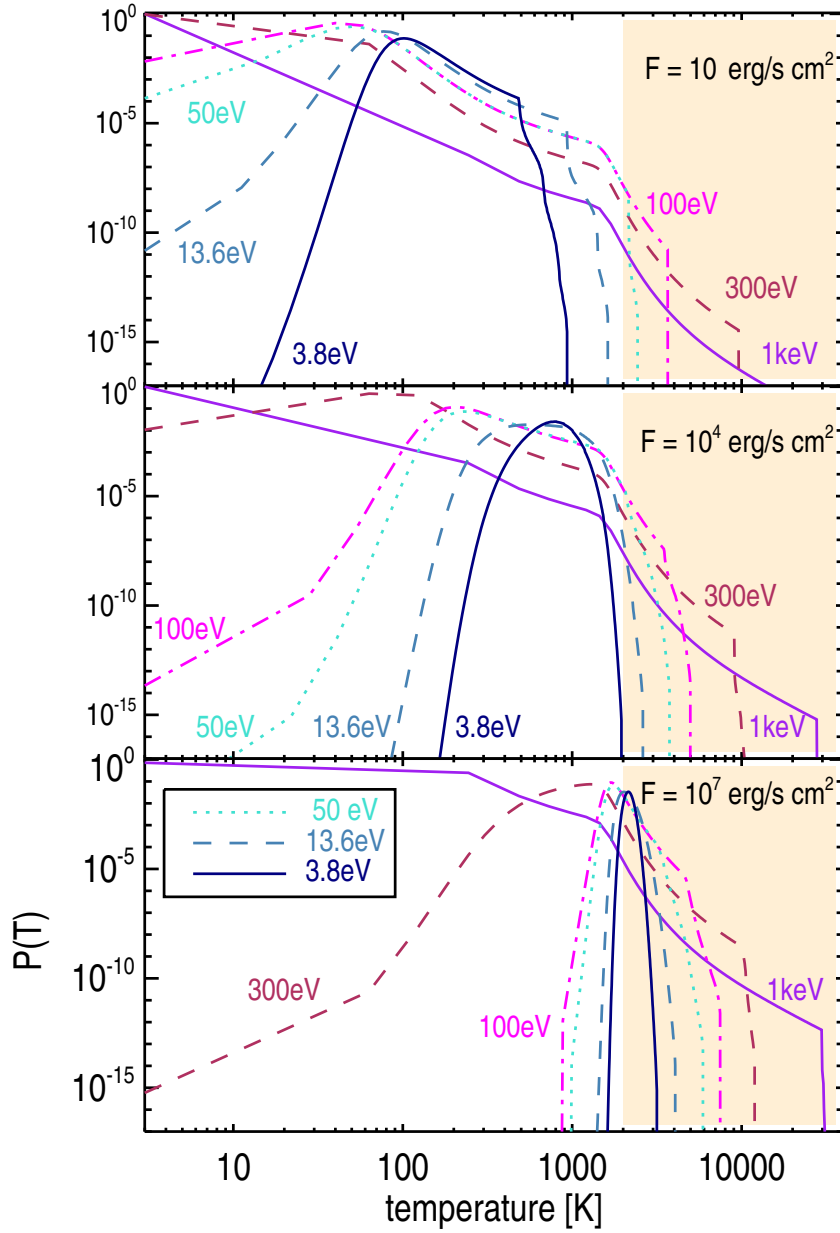


Fig. 3. The temperature distribution $P(T)$ of a PAH with 100 C atoms exposed to mono-chromatic radiation with $h\nu = 3.8, 13.6, 50, 100, 300\text{eV}$ and 1keV . This set includes the mean photon energies of the four radiation components of the T Tauri star. The fluxes range from (top to bottom) $F = 10$ to $10^7\text{erg s}^{-1}\text{cm}^{-2}$. Shaded area marks temperatures above the sublimation temperature of graphite.

to overcome the critical internal barrier, E_0 , which is similar but not identical to the chemical binding energy. Micelotta et al. (2009b) quote E_0 of 3.2eV for H-loss, 4.2eV for C_2H_2 , 7.5eV for pure C loss and 9.5eV for C_2 . For the ISM they find $E_0 = 4.6\text{eV}$ and a somewhat larger value for PDR. The inverse of the dissociation time is the probability that a certain atom leaves the PAH per unit time.

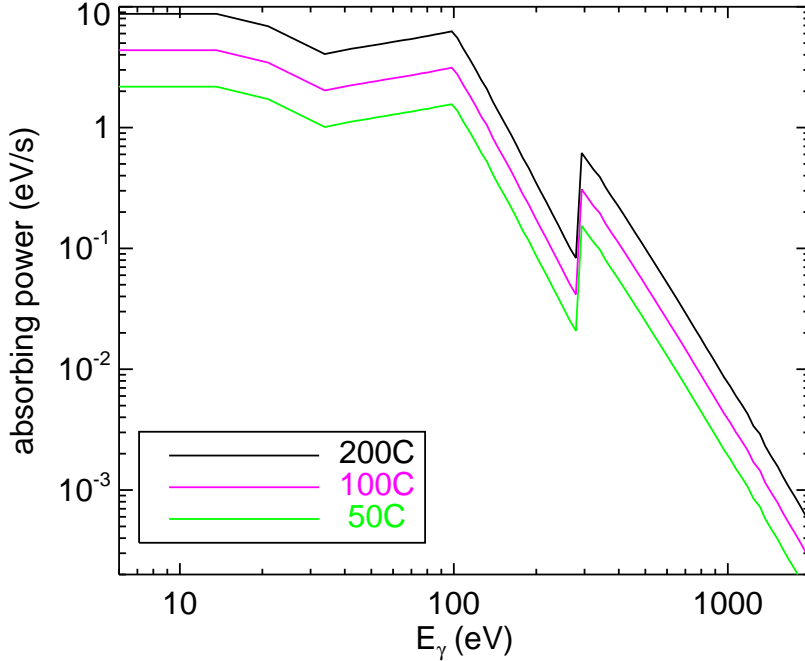


Fig. 4. The power $W = N_c \kappa F$ absorbed by one PAH, with number of C atoms N_C as indicated, in a mono-chromatic flux $F = 10^4 \text{ erg s}^{-1} \text{ cm}^{-2}$ as a function of photon energy $E_\gamma = h\nu$.

The exponential term e^{E_0/kT_p} in Eq.(7) increases very rapidly as T falls and meaningful values (i.e. not too large ones) of t_{dis} are obtained only if $T_p > 1500 \text{ K}$. Atoms will only detach when $t_{\text{dis}} < t_{\text{cool}}$. As the cooling time at these temperatures is for astrophysical applications of order 1 s, independent of the PAH size, the dissociation criterion reads

$$t_{\text{dis}} \lesssim 1 \text{ s} \quad (8)$$

It leads to a minimum temperature for destruction

$$T_{\text{dis}} = \frac{E_0}{k \ln \nu_0} \quad (9)$$

Assuming $E_0 \sim 5 \text{ eV}$, one gets $T_{\text{dis}} \simeq 2000 \text{ K}$. At this high temperature, the internal energy of a PAH is reasonably well approximated by $3N_c k T_{\text{dis}}$ when also taking the presence of H-modes into account. The minimum temperature T_{dis} is related to a minimum energy input ΔE . The PAH is therefore unstable to photons with

$$\Delta E \geq h\nu_c = 3N_c k T_{\text{dis}} = \frac{3}{\ln \nu_0} N_c E_0 \simeq 0.1 N_c E_0 \quad (10)$$

or when the number of carbon atoms

$$N_c \leq \frac{2\Delta E}{[\text{eV}]} \quad (11)$$

Micelotta et al. (2009b) find that a PAH with $N_c = 50$ requires an internal energy of about $\Delta E = 24 \text{ eV}$ to dissociate, which agrees with the above estimate (Eq. 11).

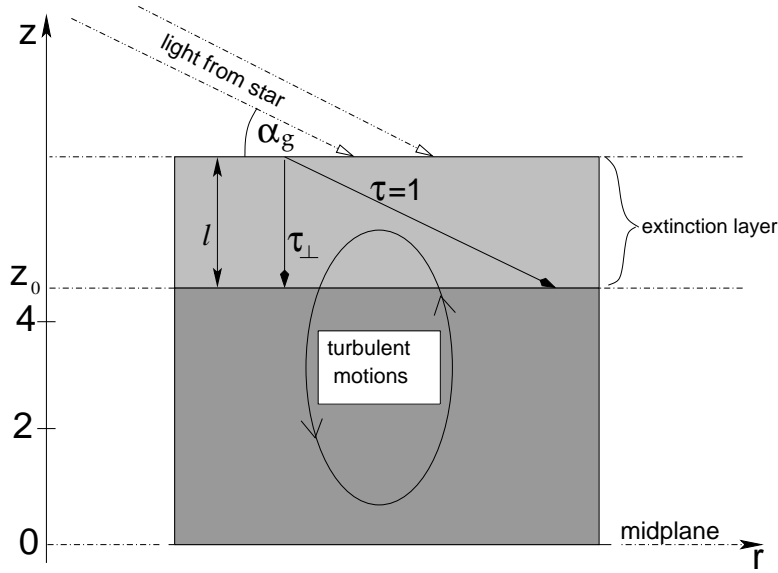


Fig. 5. Of each radiation component, $\sim 90\%$ is absorbed in what we call the extinction layer. The optical depth from its bottom to the star is one and in vertical direction equal to the grazing angle α_g . The height of its lower boundary, z_0 , declines with radius, but its geometrical thickness is rather constant ($l \sim 0.5H$, see Fig.6). Vertical motions may replenish PAHs from below.

The minimum energy input required for dissociation can either be delivered by absorption of *i*) many soft photons, with a total energy $E_{\text{abs}} \geq \Delta E$ (Eq. 3), or *ii*) by a single hard photon, with energy $h\nu \geq \Delta E$. If a photon heats the PAH to a peak temperature much above T_{dis} , more than one atom will detach. The first expulsion occurs momentarily ($t_{\text{dis}} \ll 1$ s). It consumes the energy E_0 plus some kinetic energy E_{kin} for the liberated atom. The new PAH temperature follows from

$$h\nu - E_0 - E_{\text{kin}} = 3(N_c - 1)kT \quad (12)$$

This happens x times until T has dropped to T_{dis} ,

$$h\nu - x(E_0 + E_{\text{kin}}) = 3(N_c - x)kT_{\text{dis}} \quad (13)$$

With $E_{\text{kin}} \sim 0.5$ eV, we estimate that the total number of freed atoms is

$$x = \frac{h\nu - 3N_c k T_{\text{dis}}}{E_0 + E_{\text{kin}} - 3k T_{\text{dis}}} \simeq \frac{h\nu}{5 [\text{eV}]} - \frac{N_c}{10} \quad (14)$$

For $N_c = 100$, an average EUV photon ejects nine atoms and an X-ray photon destroys the whole PAH (column (5) in Table 2).

4.2. Disruption by Coulomb forces

For completeness, we also mention disruption of PAHs by Coulomb forces. Double or multiple ionization of a PAH loosens the binding of the peripheral H atoms as well as of the skeleton of carbon atoms. The

ejection of K-shell electrons by X-ray photons ($h\nu > 284 \text{ eV}$) in combination with Auger electrons will amplify the process. Coulomb explosion is relevant mainly for small PAHs and neglected here.

5. Conditions for PAH survival

According to Eq. (10), PAHs are destroyed if the source emits photons of energy $h\nu \geq 0.1 N_c E_0$, irrespective of the distance to the star or its luminosity. For $N_c = 100$, the critical photon energy is only 50 eV (Eq.10). As T Tauri stars (or their jets) also radiate at X-rays and in the EUV, the surface of the disk should be devoid of PAHs unless *a)* the period over which hard photons are emitted is too short to destroy all PAHs; *b)* the PAHs are by vertical motions removed from the hard radiation before they are destroyed and there is an influx of PAHs from below; *c)* PAH destruction is compensated by PAH formation in the surface layer. The last effect should, in a hard photon environment where PAHs and carbon atoms are ionized, be prohibited by Coulomb repulsion (Voit, 1992).

5.1. Destruction time

The above PAH survival condition under *a)* can easily be dismissed. To estimate the time for PAH removal, t_{rem} , by the radiation component *i*, we note that most of the radiation is absorbed on the disk surface in a sheet of vertical optical depth τ_{\perp} equal to the grazing angle α_g of the incident light. We call this sheet the *extinction layer* (of radiation component *i*) and denote its geometrical thickness ℓ_i (see Fig.5). To first order, the PAHs in the extinction layer receive the stellar flux of Eq.(1) with $\tau_{\nu} = 1$. If the instability criterion of Eq.(10) is fulfilled, t_{rem} follows from $x N_{\gamma} t_{\text{rem}} = N_c$, where x is from Eq.(14), therefore

$$t_{\text{rem}} = \frac{N_c}{x} t_{\text{abs}} \quad (15)$$

With t_{abs} from Table 2, one sees that even at 100 AU, t_{rem} is short compared to the duration of the T Tauri phase ($\sim 10^6$ yr, Bertout et al. 2007, Cieza et al. 2007).

5.2. Exposure time and vertical mixing

Next we consider the possibility that vertical motions in the disk lead to a continuous exchange between matter in the extinction layers, where almost all photons are absorbed and PAHs destroyed, and the layers below where PAHs are shielded and damaged ones possibly rebuilt (Fig.5). We assume that gas and dust are perfectly mixed in a mass ratio 130:1.

In a Keplerian disk that is isothermal in z -direction and in hydrostatic equilibrium, the gas density changes like

$$\rho(z) = \sqrt{\frac{2}{\pi}} \frac{\Sigma}{H} e^{-z^2/2H^2} \quad (16)$$

Here $\Sigma(r)$ is the surface density at radius r which is assumed to follow a power law,

$$\Sigma(r) = \int_0^{\infty} \rho(z) dz = \Sigma_0 \left[\frac{r}{\text{AU}} \right]^{-\gamma} \quad (17)$$

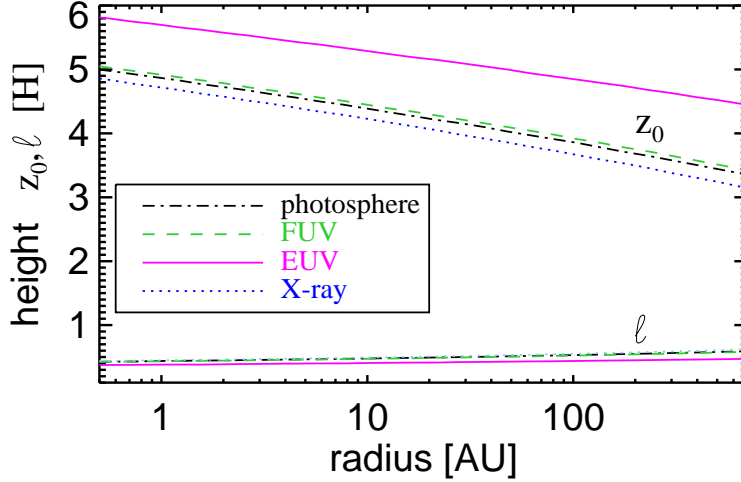


Fig. 6. The height, z_0 , of the bottom of the extinction layer and its thickness ℓ for the four radiation components (see Fig.5 and Eq.(21), (22)) for a grazing angle $\alpha_g = 3^\circ$. Due to the high gas densities, the EUV extinction layer is practically coincident with the ionization front and lies above the extinction layer of the other components. This implies that EUV radiation is absorbed first whereas the other components penetrate deeper. Neglecting ionization by the FUV component, the gas below the z_0 -line of the EUV radiation (top) is neutral.

and

$$H(r) = \sqrt{kTr^3/GM_*m} \quad (18)$$

is the scale height, $M_* \simeq 1 M_\odot$ the stellar mass and m the mass of a gas molecule. For the surface density, reasonable numbers are $\gamma = 1$ and $\Sigma = 200 \text{ g cm}^{-2}$ (Hartmann et al. 1998, Kitamura et al. 2002, Dullemond et al. 2002, Rafikov & Colle 2006, Gorti & Hollenbach 2008), although the various estimates show considerable scatter.

For the radial variation of the gas temperature in the opaque mid plane, $T(r)$, we also adopt a power law,

$$T(r) = T_0 \left[\frac{r}{\text{AU}} \right]^{-\beta} \quad (19)$$

The mid plane is roughly isothermal in z because the optical depth is high and the net flux zero. It is much colder than the extinction layers because it is not exposed to direct stellar heating. The radiative transfer in the disk, including the energy equation, can be solved to any desired accuracy even when the disk is very opaque (see section 11.3.2 of Krügel 2006). As long as the dust in the mid plane is optically thick to its own emission, the results for $T(r)$ can be well approximated by putting in Eq.(19) $\beta = 0.5$ and $T_0 \sim 130 \text{ K}$ (as also suggested by Dullemond et al. 2007b or Chiang & Goldreich 1997).

Each extinction layer extends vertically from some value z_0 upwards to infinity (Fig.5). We give it a finite thickness ℓ by demanding that, say, 90% of the photons are absorbed between z_0 and $z_0 + \ell$. If v_\perp

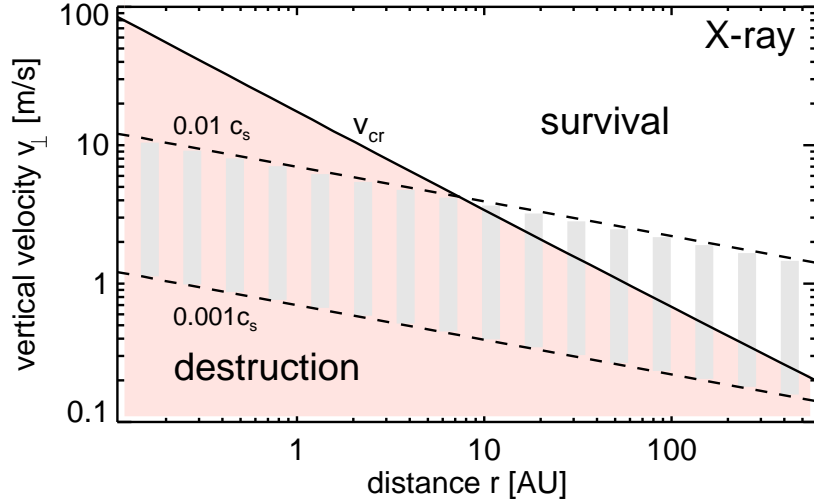


Fig. 7. The critical vertical velocity for PAH survival v_{cr} after Eq. (23) with respect to X-rays as a function of distance (full line). We identify the vertical velocity v_{\perp} with the turbulent velocity v_t . PAHs survive when $v_{\perp} = v_t > v_{\text{cr}}$, else they are destroyed (shaded areas) by expulsion of atoms. The hatched strip between the dashed lines shows the range where v_{\perp} is between $0.001 c_s$ and $0.01 c_s$ (where c_s is the sound velocity).

denotes the typical vertical velocity, for example, as a result of turbulence, PAHs are exposed to radiation for a time

$$t_{\text{exp}} = \frac{\ell}{v_{\perp}} \quad (20)$$

This is also the mean residence time of a PAH in the extinction layer. For PAHs to survive, t_{exp} must be smaller than t_{rem} Eq.(15). The height z_0 follows from

$$K \int_{z_0}^{\infty} \rho(z) dz = \alpha_g \quad (21)$$

and ℓ may be estimated from the condition that only 10% of the flux is absorbed above $z_0 + \ell$,

$$K \int_{z_0+\ell}^{\infty} \rho(z) dz = 0.1 \alpha_g \quad (22)$$

K is the mass absorption coefficient of gas and dust at the characteristic frequency of the particular radiation component (see Table 2). Because $\rho(z)$ changes rapidly, z_0 is rather insensitive both to α_g as well as K . For $\alpha_g/K = 10^{-8} \dots 10^{-2}$, one obtains $z_0 = 2.6H \dots 5.7H$. So in the V band, where absorption is only by dust ($K \simeq 200 \text{ cm}^2 \text{ g}^{-1}$) and for a grazing angle $\alpha_g = 3^\circ$, one gets $z_0 \simeq (4 \dots 5)H$ and $f_{\ell} = \ell/H \simeq 0.5$. The height z_0 where an extinction layer begins and its thickness are shown in Fig.6; ℓ is for all radiation components very similar ($\ell_i \sim H/2$, $i = 1, \dots, 4$). EUV photons are absorbed highest up, their extinction layer lies about one scale height above the others. X-rays penetrate slightly deeper than photospheric or FUV photons.

Table 2. Quantities relevant to PAH survival.

	(1)	(2)	(3)	(4)	(5)	(6)	(7)	(8)	(9)
component	$h\bar{\nu}$ eV	κ 10^{-4}\AA^2	η	K/K_V	x	z_0/H	ℓ/H	t_{abs}	v_{cr} m/s
photosphere	2.7	700	$\ll 1$	1.2	-	4.4	0.5	5 s	-
FUV	4.2	700	$\ll 1$	1.5	-	4.5	0.5	120 s	-
EUV	97	36	~ 0.5	110	9	5.3	0.4	9 days	2900
X-ray	1100	0.17	$\ll 1$	0.55	100	4.2	0.5	290 yr	3.4

(1) The mean energy of destructive photons, $h\bar{\nu}$, from Eq.(5) at the bottom of the extinction layer (see Fig.5); for photospheric and FUV photons we put $\nu_c = 0$ and for EUV and X-rays we integrate for $\nu \geq \nu_c$ (Eq. 10);

(2) absorption cross section, κ , per C atom at frequency $\bar{\nu}$;

(3) approximate mean degree of ionization of the gas in the extinction layer;

(4) extinction cross section of gas and dust at frequency $\bar{\nu}$ normalized to $K_V = 200 \text{ cm}^2 \text{ g}^{-1}$;

(5) number of expelled atoms, x , per absorption event from Eq.(14);

(6) altitude of the bottom of the extinction layer in units of the scale height H ;

(7) thickness of extinction layer;

(8) mean time t_{abs} from Eq.(4) in which one photon is absorbed;

(9) critical vertical velocity for PAH survival.

Note: $z_0, \ell, t_{\text{abs}}$ and v_{cr} refer to $r = 10 \text{ AU}$.

From Eq.(4), (15) and (20), one finds that vertical motions safeguard PAHs against destruction if

$$v_{\perp} > v_{\text{cr}} = \frac{\ell x}{t_{\text{abs}} N_c} = \frac{f_{\ell} H x}{4\pi r^2} \int_{\nu_c}^{\infty} \frac{L_{\nu} e^{-\tau_{\nu}} \kappa_{\nu}}{h\nu} d\nu \quad (23)$$

with ν_c from Eq.(10). When the scale height H is given by Eq.(18), $v_{\text{cr}} \propto r^{-(\beta+1)/2} = r^{-3/4}$. The values of v_{cr} , at a distance of 10 AU, are listed in Table 2 together with other quantities relevant to PAH survival.

One expects the disk also to be turbulent. Turbulence may be driven by various processes such as shear flows in the disk (Lin & Bodenheimer 1982), magneto-rotational instabilities (Balbus & Harley 1991) or velocity discontinuities at places where infalling matter (Cassen & Mossman 1981) or outflows (Elmegreen 1978) strike the disk surface. Until now it is not clear which type of turbulence dominates. We assume that for the size of the largest Eddies, ℓ_{ed} , the average turbulent velocity, v_t , grows linearly with the sound speed c_s . Various hydrodynamical 3-dimensional calculations (Cabot 1996, Boss 2004, Johansen & Klahr 2005, Fromang & Papaloizou 2006) support this view. The favoured parametrisation is $v_t = \alpha^q c_s$ with $q = 0.5$. This choice has consequences on the Eddy scale $\ell_{\text{ed}} = \alpha^{1-q} H$ and the turn over time $t_{\text{ed}} = \ell_{\text{ed}}/v_t = \alpha^{1-2q}/\Omega_K$, with Kepler frequency $\Omega_K = \sqrt{GM_*/R^3}$ (e.g. Dullemond & Dominik 2004). Weidenschilling & Cuzzi (1993) use $q = 1$ so that the Eddy scale is about the pressure scale height, $\ell_{\text{ed}} = H$, and larger than the thickness of the extinction layer, $\ell_{\text{ed}} > \ell \sim H/2$. Estimated values for α are in the range from 0.0001 up to 0.1 (Dullemond & Dominik 2004, Schr apler & Henning 2004, Youdin & Lithwick 2007). Taking $\alpha = 0.01$ the Eddy scale is 10 times smaller for $q = 0.5$ than for $q = 1$, and

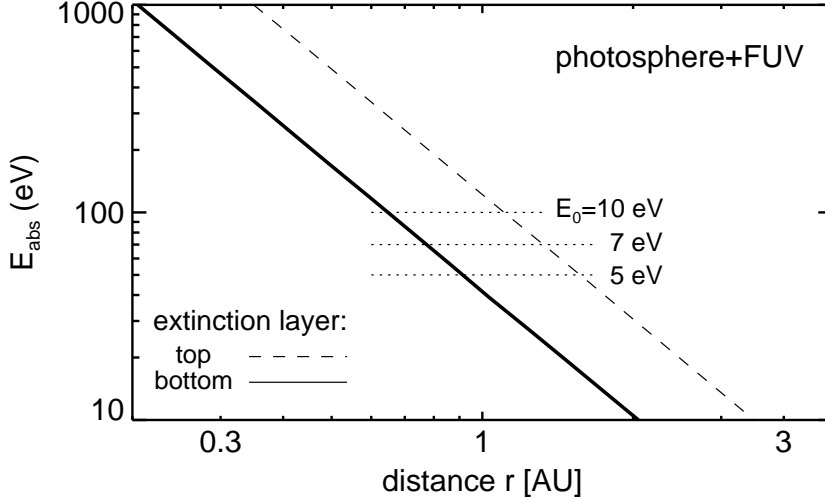


Fig. 8. The energy E_{abs} (Eq.3), which is absorbed by a PAH of $N_c = 100$ carbon atoms, as a function of distance from the star. The PAH is exposed to the photospheric and FUV radiation component described in Table 1. The dashed line refers to the top of the extinction layer ($\tau = 0$) and the full line to its bottom ($\tau = 1$). For Arrhenius energy of $E_0 = 5, 7$ and 10 eV, the minimum energy input ΔE (Eq.10) for PAH dissociation is indicated by the dotted lines.

in addition larger turbulent velocities are obtained with $v_t = \sqrt{a}c_s$, supporting a faster transport of the PAH. Identifying v_{\perp} in Eq.(23) with the turbulent velocity v_t and assuming a temperature dependence as in Eq.(19), we plot in Fig.7 the vertical velocity v_{\perp} as a function of radius. The figure also shows the critical velocity for PAH survival, v_{cr} , with respect to X-rays. Note that the critical velocity is for the X-ray radiation component insensitive to the particular choice of E_0 and ν_c (Eq. 10, 23). When $v_{\perp} = 0.01 c_s$, PAHs can survive at distances $r > 10$ AU; when v_{\perp} is considerably smaller than $0.01 c_s$, they cannot.

Critical velocities for PAH survival are much higher for EUV than for X-ray photons (Table 2). EUV radiation will therefore always destroy PAHs but, as depicted in Fig.6, the EUV extinction layer is the topmost and below it, PAHs may survive and be excited.

If PAHs are removed from the extinction layer before they are destroyed, they must, in order to be detected, at the same rate be injected from below. Therefore, the critical velocity can alternatively be expressed through

$$\frac{1}{t_{\text{rem}}} \int_{z_0}^{z_0+\ell} \rho(z) dz \simeq \rho(z_0) v_{\text{cr}} \quad (24)$$

which leads to similar values. We note that the mass reservoir below the extinction layer is sufficient to sustain, over the lifetime of the disk t_{life} , the required mass influx ρv_{cr} .

5.3. PAH dissociation by soft versus hard photons

The energy E_{abs} (Eq.3), which is absorbed by a PAH of $N_c = 100$ carbon atoms, is shown in Fig. 8 as a function of distance from the star. The PAH is exposed to the photospheric and FUV radiation component described in Table 1 and results are shown for the top ($\tau = 0$) and the bottom ($\tau = 1$) of the extinction layer. The minimum energy input ΔE (Eq.10) for PAH dissociation depends on the choice of the Arrhenius energy E_0 and is indicated for $E_0 = 5, 7$ and 10 eV, respectively. In this picture, for $E_0 = 5$ eV and at the bottom of the extinction layer, PAHs are dissociated by soft photons up to 1 AU. For X-rays, however, we find that PAH destruction occurs typically at distances up to ~ 10 AU or even larger (Fig.7). Dissociation of PAH acts for soft (photospheric and FUV) photons on much shorter distances than for hard photons (X-ray component).

6. Large grains

Observations of T Tauri stars at millimeter wavelengths (Testi et al. 2003, Lommen et al. 2007) and in the mid infrared (van Boekel et al. 2003, Przygodda et al., 2003, Kessler-Silacci et al. 2006, Bouwman et al. 2008, Watson et al. 2009) suggest that grains in T Tauri disks are at least 10 times larger than those in the ISM. As such large grains may also be present in the top disk layer we estimate how this would affect the stability analysis of PAHs. We first note that in case of homogeneous mixing an increase in particle size would not alter the dust-to-gas mass ratio.

Should the grains be much larger than the wavelength, the absorption coefficient per gram of dust, $K_{d,\lambda}$, would decrease roughly like one over grain radius whereas the ratio $K_{d,\lambda}/K_{d,V}$ would still roughly be given by the values in Table 2. For hard X-rays, on the other hand, $K_{d,\lambda}$ is not sensitive to grain size.

Therefore, if disk grains are on average ten times bigger and thus 10^3 more massive than interstellar ones, we expect that the height z_0 to which the stellar radiation components can penetrate (see Fig.6) stays the same for X-rays, but also for EUV radiation because EUV absorption is due to gas, not dust. However, optical and FUV photons will reach farther down, about half a scale height, so that there may be a thin disk layer ($\sim H/4$) where PAHs are shielded from X-rays and EUV photo-destruction and excited by optical or FUV radiation.

7. Conclusion

In the search for an explanation why most T Tauri stars do not exhibit PAH features and only a few do, we investigate which processes can remove PAHs from the surface layer of T Tauri disks and under which conditions they should be present. Clearing of PAH through interaction with planets seems not an efficient process (Geers et al 2007b) and we show that PAH under-abundance can be caused by radiative destruction. We use a fiducial model for the photon emission of the T Tauri star that includes, beside the photosphere, FUV and EUV radiation and an X-ray component.

1. We introduce for each stellar radiation component the notion of *extinction layer* as the place where $\sim 90\%$ of the photons are absorbed. EUV photons are mainly absorbed by gas, X-rays by gas and dust alike and the photospheric and FUV component are only attenuated by dust. The extinction layer of

- all four components have a similar geometrical thickness and their bottom is at similar elevation z_0 , except for the EUV extinction layer which lies higher up (Fig.6).
2. PAH may be radiatively destroyed, by unimolecular dissociation, where one or several atoms are expelled after photon absorption.
 3. Destruction by the photospheric and FUV radiation component (soft photons), increases with the strength of the radiation field and is very efficient below 1 AU.
 4. Hard photons can dissociate PAHs at all distances and their efficiency grows with the hardness of the photons. Without some counter process, all PAHs (in layers where they can be excited) would be destroyed within a time short compared to the lifetime of the disk.
 5. Although grains in the disk surface are presumably larger than interstellar ones, the stability analysis of PAHs would not change significantly.
 6. Therefore, in disks where PAHs are detected, there must be some survival channel. Because creation of PAHs in the extinction layer is too slow to compete with PAH destruction (Voit 1992), we suggest *vertical mixing* as a result of turbulence. It can replenish PAHs or remove them from the reach of hard photons.
 7. For standard disk models, the minimum velocity for PAH survival is proportional to $r^{-3/4}$ and equals ~ 5 m/s at 10 AU. If turbulent velocities are proportional to the sound speed a velocity $v_t \geq 5$ m/s would imply $v_t/c_s \gtrsim 0.01$ as PAH survival condition. Theoretical predictions for this ratio have a large spread but in accordance with the observational fact that PAH features are usually absent it seems that generally the condition is not fulfilled.
 8. A higher PAH detection rate is found in Herbig Ae/Be stars. In our picture this is explained as their destructive hard radiation component is relatively weak ($L_x/L_* \lesssim 10^{-7}$, Preibisch et al. 2006) and because the intensity of the PAH emission from large distance from the star is larger given their higher optical luminosities.

Acknowledgements. We thank the second anonymous referee for constructive comments.

References

- Akeson R.L., Walker C. H., Wood K., et al., 2005, ApJ 622, 440
 Allamandola L.J., Tielens A.G.G.M., Barker J.R., 1989, ApJS 71, 733
 Acke B., & van den Ancker, 2004, A&A 426, 151
 Balbus S.A., Hawley J.F., 1991, ApJ 376, 214
 Boss A.P., 2004, ApJ 610, 456
 Brown J.M., Blake G.A., Qf C., Dullemond C.P., Wilner D.J., 2008, ApJ, L109
 Balucinska-Church M., & McCommon D., 1992, ApJ 400, 699
 Bertout C., Siess L., Cabrit S., 2007, A&A 473, L21
 Bouwman J., Henning Th., Hillenbrand L.A., 2008, ApJ 683, 479
 Cabot W., 1996, ApJ 465, 874
 Calvet N., Gullbring E., 1998, ApJ 509, 802
 Cassen P.M., Mossman A., 1981, Icarus 48, 353
 Chiang E.I., Goldreich P., 1997, ApJ 490, 368
 Cieza L., Padgett D.L., Stapelfeldt K.R., et al., 2007, ApJ 667, 328
 CRC Handbook of Chemistry & Physics, 2005, Taylor & Francis, p.6ff

- Dullemond C.P., van Zadelhoff G.J., Natta A., 2002, A&A 389, 464
- Dullemond C.P., Dominik C., 2004, A&A 421, 1075
- Dullemond C. P., Henning Th., Visser R., et al., 2007, A&A 473, 457
- Dullemond C. P., Hollenbach D., Kamp I., D'Alessio P., 2007b, in: Protostars and Planets V, B. Reipurth, D. Jewitt, and K. Keil (eds.), University of Arizona Press, Tucson, p.555
- Dwek E., & Smith R.K., 1996, ApJ 459, 686
- Elmegreen B.G., 1978, Moon and Planets 19, 21
- Evans N.J., Allen L.E., Blake G.A., et al., 2003, PASP 115, 965
- Fromang S., Papaloizou J., 2006, A&A 452, 751
- Furlan E., Hartmann L., Calvet N., et al., 2006, ApJS 156, 568
- Geers V.C., Augereau J.-C., Pontoppidan K. M., et al., 2006, A&A 459, 545
- Geers V.C., van Dishoeck E.F., Pontoppidan K.M., et al., 2007a, A&A 476, 279
- Geers V.C., Pontoppidan K.M., van Dishoeck E.F., et al., 2007b, A&A 469, L35
- Geers V.C., van Dishoeck E.F., Pontoppidan K.M., et al., 2009, A&A 495, 837
- Güdel M., Skinner, S. L., Mel'Nikov S. Yu., 2007, A&A 468, 353
- Guhathakurta P., Draine B.T., 1989, ApJ 345, 230
- Gorti U., Hollenbach D., 2008, ApJ 683, 287
- Kassis M., Adams J.D., Campbell M.F., 2006, ApJ 637, 823
- Kessler-Silacci J., Augereau J.-C., Dullemond C., et al., 2006, ApJ 639, 275
- Kitamura Y., Momose M., Yokogawa S., et al., 2002, ApJ, 581, 357
- Krügel E., 2006 *An introduction to the Physics of Interstellar Dust*, IoP, Sect. 5.4 and 10.2
- Johansen A., Klahr H., 2005, ApJ 634, 1353
- Judge P.G., Solomon S.C., Ayres T.R., 2003, ApJ 593, 534
- Leach S., Eland J.H.D., Price S.D., 1989a, J. Phys. Chem. 93, 7575
- Leach S., Eland J.H.D., Price S.D., 1989b, J. Phys. Chem. 93, 7583
- Leger A., D'Hendecourt L., Boissel P., Desert F.X. , 1989, A&A 213, 351
- Le Page V., Snow T.P. , Bierbaum V.M., 2003, ApJ 584, 316
- Lin D.N.C., Bodenheimer P., 1982, ApJ 262, 768
- Lommen D., Wright C.M., Maddison S.T., et al., 2007, A&A 462, 211
- Meeus G., Waters L.B.F.M., Bouwman J., et al. 2001, A&A 365, 476
- Micelotta E.R., Jones A.P. and Tielens A.G.G.M., 2009a, A&A in press
- Micelotta E.R., Jones A.P. and Tielens A.G.G.M., 2009b, A&A in press
- Morrison R., & McCommon D., 1983, ApJ 270, 119
- Muzerolle J., Hartmann L. and Calvet N., 1998, AJ 116, 2965
- Muzerolle J., Calvet N., Hartmann L., D'Alessio P., 2003, ApJ 597, L149
- Omont A., 1986, A&A 166, 159
- Peeters E., Hony S., van Kerckhoven C., et al., 2002, A&A 390, 1089
- Preibisch T., Kim Y.-C., Favata F., et al., 2006, ApJSS 160, 401
- Przygodda F., van Boekel R., Abraham, P., et al., 2003, A&A 412, 43
- Rafikov R.R., de Colle, F., 2006, ApJ 646, 275
- Rapacioli M., Calvo F., Joblin C., et al., 2006, A&A 460, 519
- Ruhl E., Price S.D., Leach S., 1989, J. Phys.Chem. 93, 6312
- Salpeter E.E., 1977, ARA&A 15, 267
- Schräpler R., Henning Th., 2004, ApJ 614, 960
- Schutte W. A., Tielens A. G. G. M. and Allamandola L. J., 1993, ApJ 415, 397
- Siebenmorgen R., Prusti T., Natta A., Müller T.G., 2000, A&A 361, 258
- Stahler S.W., Shu F.H., Taam R.E., 1980 ApJ 242, 226
- Stelzer B., Micela G., Hamaguchi K., Schmitt J.H.M.M., 2006, A&A 457, 223
- Stelzer B., Flaccomio E., Briggs K., 2007, A&A 468, 463

- Sterzik M.F., Schmitt H.M.M., 1997, *AJ* 114 (4), 1673
- Testi L., Natta A., Shepherd D.S., Wilner D.J., 2003, *A&A* 403, 323
- Tielens A.G.G.M., 2005, *The Physics and Chemistry of the Interstellar Medium*, ISBN 0521826349, Cambridge University Press, Sect. 6.4
- Tielens A.G.G.M., 2008, *ARA&A* 46, 289
- Visser R., Geers V. C., Dullemond C. P., et al., 2007, *A&A* 466, 229
- Voit G.M., 1992, *MNRAS* 258, 841
- van Boekel R., Waters L.B.F.M., Dominik C., et al., 2003, *A&A* 400, 21
- van Boekel R., Min M., Leinert C., et al., 2004, *Nature* 432, 479
- Waelkens C., Waters L.B.F.M., de Graauw M.S., et al., 1996, *A&A* 315, L245
- Watson D.M., Leisenring J.M., Furlan E., et al., 2009, *ApJS* 180, 84
- Weidenschilling S.J., Cuzzi J.N., 1993, *Protostars and Planets III* (A93-42937 17-90), p. 1031-1060.
- Youdin A.N., Lithwick Y., 2007, *Icar* 192, 588

PAH destruction and survival in the disks of T Tauri stars

R. Siebenmorgen¹ and E. Krügel²

¹ European Southern Observatory, Karl-Schwarzschildstr. 2, D-85748 Garching b. München, Germany

² Max-Planck-Institut für Radioastronomie, Auf dem Hügel 69, Postfach 2024, D-53010 Bonn, Germany

Received Month XX, 2009 / Accepted Month XX, 20XX

ABSTRACT

In Spitzer observations of Tauri stars and their disks, PAH features are detected in less than 10% of the objects, although the stellar photosphere is sufficiently hot to excite PAHs. To explain the deficiency, we discuss PAH destruction by photons assuming that the star has beside its photospheric emission also a FUV, an EUV and an X-ray component with fractional luminosity of 1%, 0.1% and 0.025%, respectively. As PAH destruction process we consider unimolecular dissociation and present a simplified scheme to estimate the location from the star where the molecules become photo-stable. We find that soft photons with energies below ~ 20 eV dissociate PAHs only up to short distances from the star ($r < 1$ AU); whereas dissociation by hard photons (EUV and X-ray) is so efficient that it would destroy all PAHs (from regions in the disk where they could be excited). As a possible path for PAH survival we suggest turbulent motions in the disk. They can replenish PAHs or remove them from the reach of hard photons. For standard disk models, where the surface density changes like r^{-1} and the mid plane temperature like $r^{-0.5}$, the critical vertical velocity for PAH survival is proportional to $r^{-3/4}$ and equals ~ 5 m/s at 10 AU which is in the range of expected velocities in the surface layer. The uncertainty in the parameters is large enough to explain both detection and non-detection of PAHs. Our approximate treatment also takes into account the presence of gas which, at the top of the disk, is ionized and at lower levels neutral.

Key words. dust, extinction – planetary systems: protoplanetary disks – infrared: stars – X-rays: stars – X-rays: ISM

1. Introduction

Infrared emission bands of PAHs can be used as a probe of the UV environment. They are commonly seen in the ISM, but also in young stellar objects such as Herbig Ae/Be stars (Waelkens et al. 1996, Siebenmorgen et al. 2000, Meeus et al. 2001, Peeters et al. 2002, van Boekel et al. 2004). The observed emission can be explained in models of an irradiated disk (Habart et al. 2004, Visser et al., 2007, Dullemond et al. 2007a).

ISO also looked at a few of the much fainter T Tauri stars but without a clear PAH detection (Siebenmorgen et al. 2000). In the Evans et al. (2003) legacy program which employs the more sensitive Spitzer Space Telescope (SST), 3 out of 38 T Tauri stars show PAH features (Geers et al. 2006). This corresponds to a detection rate of only 8% in contrast to almost 60% in Herbig Ae/Be stars (Acke & van den Ancker 2004). Similarly low rates for T Tauri stars are found by Furlan et al. (2006) who present 111 SST spectra in the Taurus-Auriga star forming region and speculate

that the absence of PAH resonances is due to the much weaker UV field compared to Herbig Ae/Be stars. Geers et al. (2009), on the other hand, argue that the PAHs are simply under-abundant relative to the ISM. They also find that variations of the disk geometry, such as flaring or gaps, have only a small effect on the strength of the PAH bands. Clearing out gas and dust by planet formation inside the disk could effectively remove PAHs. Indeed, inner gaps in disks are observed at radii between 40–60 AU and at wavelengths between 20–1000 μ m where the emission is dominated by large grains (Brown et al. 2008, Geers et al. 2007b). However, in cases where PAH emission is resolved, it is extended up to 15–60 AU, without sub-structure and inside the inner gap region (Geers et al. 2007a). The spatial extent of the PAH emission is also similar for T Tauri and Herbig Ae/Be stars. We therefore suggest that PAH removal by radiative destruction is dominant.

Present radiative transfer models of the PAH emission from dusty disks consider only the stellar radiation field and no additional EUV or X-ray component (Habart et al. 2004, Geers et al. 2006,

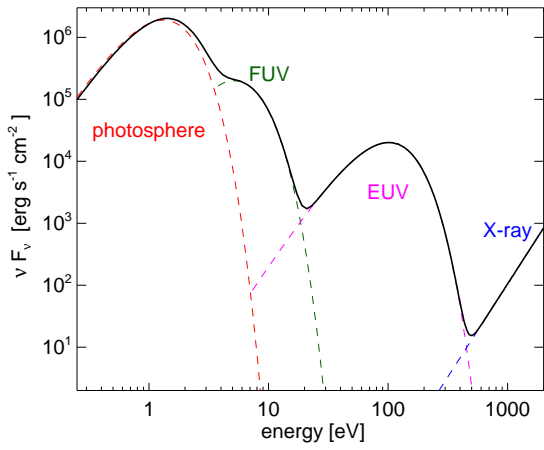


Fig. 1. The spectral energy distribution of our T Tauri model star at 1 AU without foreground extinction (Eq. 1). The absolute luminosities of the components are given in Table 1.

Visser et al. 2007, Dullemond et al. 2007). Their hard photons could, according to laboratory experiments (Ruhl et al. 1989, Leach et al. 1989a,b, Jochims et al. 1994) and theory (Omont 1986, Tielens 2005, Rapacioli et al. 2006, Micelotta et al. 2009), destroy PAHs. We discuss below their impact on the PAH abundance in the disks of T Tauri stars.

2. Radiation components of T Tauri stars

Our T Tauri model star has a total luminosity $L_* = 2 L_\odot$. Its radiation consists of a photospheric, a FUV, an EUV and an X-ray component. Their parameters are listed in Table 1 and are very similar to those proposed by Gorti & Hollenbach (2008). The total spectrum is displayed in Fig.1. We point out that the FUV and EUV radiation are observationally poorly constrained.

The photosphere supplies most of the luminosity whereas the FUV, EUV and X-ray radiation are much weaker and believed to originate from accretion onto the star and from chromospheric and coronal activity. The photosphere, the FUV and EUV component are approximated by blackbodies. We assume 4000 K for the photosphere and, following Stahler et al. (1980) and Calvet & Gullbring (1998), 15000 K for the FUV (pre-shock) and $\sim 3 \times 10^5$ K for the EUV emission (post-shock region).

The strength of the FUV and EUV radiation is determined by the accretion luminosity which we approximate by $L_{\text{acc}} = GM_* \dot{M} / R_*$. If $R_* = 2 R_\odot$ and $M_* = 1 M_\odot$ are the radius and mass of the star, an accretion rate $\dot{M} = 10^{-9} M_\odot \text{ yr}^{-1}$ (Akeson et al. 2005) yields $L_{\text{acc}} \sim 0.01 L_*$. Higher values

($L_{\text{acc}}/L_* \gtrsim 0.1$), but with a large spread, are derived by Muzerolle et al. (1998, 2003) from hydrogen emission lines. However, as we show in section 5, such stronger fluxes have little influence on the stability analysis of PAHs.

Preibisch et al. (2006) establish from Chandra observations (0.5–8 keV) a relation between the X-ray luminosity, L_x , and the total luminosity L_* confirming the ROSAT results of Sterzik & Schmitt (1997). The ratio L_x/L_* is similar in rapidly rotating main-sequence stars and non-accreting T Tauri stars ($\sim 10^{-3}$), but systematically lower by a factor ~ 4 in accreting T Tauri stars (Preibisch et al. 2006). Interestingly, in Herbig Ae/Be stars L_x/L_* is much smaller ($\sim 10^{-7} \dots 10^{-5}$, Stelzer et al. 2006) with values comparable to the Sun. The solar X-ray luminosity in the 0.1–2.4 keV ROSAT passband lies during a solar cycle in the range $10^{-6.8} \lesssim L_x/L_* \lesssim 10^{-5.7}$ and is typical for G stars (Judge et al. 2003).

X-ray fluxes are generally variable on timescales of hours to weeks and weaken during the evolution of the T Tauri star. For example, half of the sources in the Taurus molecular cloud detected by XMM/Newton (0.3 – 7.8 keV) show variations, more at hard (> 0.5 keV) than at soft energies, and a quarter of them display flares (Stelzer et al. 2007), about once a week and lasting for a few hours. In a strong flare, more than 10^{35} erg are emitted and L_x can reach 1% of the total luminosity. We assume up to 2 keV a power law spectrum $\propto \nu^2$ (Güdel et al. 2007) and neglect harder radiation because the emission then steeply declines ($\propto \nu^{-3}$).

Let L_i be the frequency-integrated luminosity of the radiation component i (see Table 1) and $L_{i,\nu}$ its spectral luminosity such that $L_i = \int L_{i,\nu} d\nu$. Dropping for convenience the index i , the flux (of component i) at a distance r is

$$F_\nu = \frac{L_\nu e^{-\tau_\nu}}{4\pi r^2} \quad (1)$$

where we included a screening factor $e^{-\tau_\nu}$ to account for foreground absorption (by dust and gas). If κ_ν denotes the absorption cross section per carbon atom, a PAH of N_c carbon atoms absorbs in one second (from component i)

$$N_\gamma = N_c \int \frac{F_\nu \kappa_\nu}{h\nu} d\nu \quad (2)$$

photons of total energy

$$E_{\text{abs}} = N_c \int F_\nu \kappa_\nu d\nu \quad (3)$$

The inverse of N_γ is the average time between two absorption events,

$$t_{\text{abs}} = N_\gamma^{-1} \quad (4)$$

The mean photon energy equals

$$h\bar{\nu} = \frac{\int F_\nu \kappa_\nu d\nu}{\int \frac{F_\nu \kappa_\nu}{h\nu} d\nu} \quad (5)$$

Table 1. The four radiation components of our T Tauri model star.

		(1)	(2)	(3)	(4)
i	component	L/L_*	spectrum	$h\bar{\nu}_{\text{em}}$ (eV)	F_{10} ($\text{erg s}^{-1}\text{cm}^{-2}$)
1	photosphere	0.99	4000 K BB	0.9	30 000
2	FUV	0.01	15000 K BB	3.5	300
3	EUV	0.001	3×10^5 K BB	70	30
4	X-rays ($h\nu < 2\text{keV}$)	2.5×10^{-4}	$\propto \nu^2$	1330	10

- (1) fractional luminosity,
(2) spectral shape (BB = blackbody),
(3) mean energy of emitted photons, $h\bar{\nu}_{\text{em}}$,
(4) approximate flux at 10 AU, F_{10} .

3. Cross sections

As the light from the star enters the disk, it is attenuated by gas and dust. The absorption cross section of gas depends on the ionization stage of the atoms which is determined by the balance between recombination and photo-ionization. By far the most important atoms are, of course, hydrogen and helium with ionization potentials of 13.6 eV and 24.6 eV, respectively. Because the recombination rate is proportional to the square of the gas density which is high in the disk (section 5), the gas is ionized only in a thin surface layer ($A_V < 0.001$ mag, section 2.6 of Gorti & Hollenbach 2008). We use atomic cross sections of Morrison & McCommon (1982) and Balucinska-Church & McCommon (1992) and solar element abundances.

The dust cross sections are taken from the model of Krügel (2006) which describes standard dust. For X-rays, the absorption efficiency calculated from Mie theory must be corrected downwards. Hard photons can eject electrons from the grain and as these carry away kinetic energy, only part of the photon energy is deposited in the dust particle. The threshold, E_t , above which such a correction is necessary depends on the grain size; details are given in Dwek & Smith (1996). For a 10 Å graphite particle, $E_t \sim 100$ eV and the reduction factor is roughly proportional to ν^{-1} .

The absorption coefficient of dust, $K_{d,\lambda}$, and of neutral gas plus dust, $K_\lambda = K_{\text{gas},\lambda} + K_{d,\lambda}$, both per gram of disk material, are plotted in Fig. 2 for a dust-to-gas mass ratio of 1:130. Note that at the ionization threshold of hydrogen, K_{gas} is almost 10^4 times greater than K_d .

With respect to the absorption cross section of PAHs, we assume $\kappa_\nu = 7 \times 10^{-18} \text{cm}^2$ per carbon atom when $h\nu < 13.6$ eV and scale κ_ν at higher energies to follow the values of a graphite sphere of 10 Å radius (Dwek & Smith 1996). The maximum wavelength (in Å) for PAH excitation is $\lambda_{\text{max,PAH}} = 1630 + 370\sqrt{N_c}$ (Schutte et al. 1993) resulting in a minimum photon energy of 2.3 eV for a PAH with $N_c = 100$ carbon atoms.

3.1. PAH emission

As the PAHs are transiently heated, their excitation is usually treated statistically. Following Guhathakurta & Draine (1989), let $P(T) dT$ be the probability of finding in a large ensemble of PAHs in a steady state an arbitrary PAH in the temperature interval $[T, T + dT]$. The temperature distribution function $P(T)$ is calculated in this method from a transition matrix (A_{fi}). If K_ν denotes the PAH absorption cross section, the matrix element A_{fi} referring to dust heating from an initial enthalpy bin centered at U_i to a final one centered at U_f and of width ΔU_f is, for a mono-chromatic flux, equal to

$$A_{fi} = \begin{cases} \frac{K_\nu F}{h\nu} & : \text{ if } |U_f - U_i - h\nu| \leq \frac{1}{2}\Delta U_f \\ 0 & : \text{ else} \end{cases} \quad (6)$$

Examples of $P(T)$ are displayed in Fig. 3 for mono-chromatic fluxes which cover almost the entire range encountered anywhere in the disk in terms of intensity, the flux ranges from $F = 10$ to $10^7 \text{erg s}^{-1}\text{cm}^{-2}$, as well as hardness, the photon energy is between $h\nu = 3.8$ eV and 1 keV. The approximate unattenuated fluxes of the four radiation components at a distance of 10 AU are listed in Table 1. Note that when $F = n_\gamma h\nu$ is constant, the number of photons n_γ decreases as the photon energy $h\nu$ goes up. **The power absorbed by one PAH is almost independent of the photon energy as long as $h\nu \lesssim 100$ eV (see Fig. 4).** By and large, when $h\nu$ is fixed and F increases, the curves in Fig. 3 narrow and move to the right towards higher temperatures. When the radiation field is weak ($F = 10 \text{erg s}^{-1}\text{cm}^{-2}$) and the photons are soft ($h\nu = 3.8$ eV), the PAH absorbs about one photon per day and there is plenty of time to cool down. In this case, the PAH virtually never exceeds the sublimation temperature T_s , (at which solid carbon gasify). For a wide pressure range ($10^{-1} - 10^{-7} \text{dyn cm}^{-2}$), $T_s \sim 2000$ K for graphite (CRC Handbook of Chemistry & Physics 2005, Salpeter et al. 1977). In Fig. 3 we highlight the area where the temperature is above T_s . For a PAH exposed to a strong

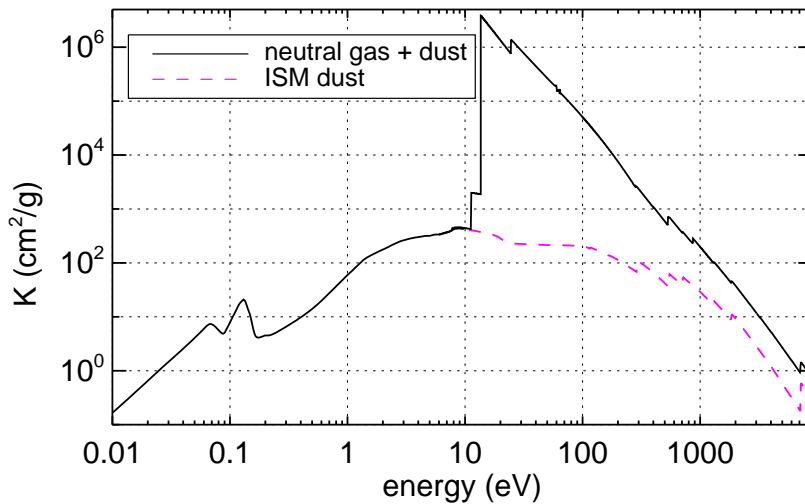


Fig. 2. The mass extinction coefficient per gram disk material when the gas is neutral (Morrison & McCommon 1983); the gas-to-dust mass ratio equals 130.

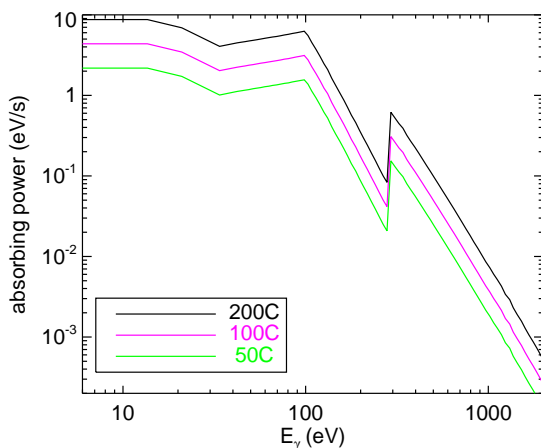


Fig. 4. The power $W = N_C \kappa F$ absorbed by one PAH, with number of C atoms N_C as indicated, in a monochromatic flux $F = 10^4 \text{ erg s}^{-1} \text{ cm}^{-2}$ as a function of photon energy $E_\gamma = h\nu$.

radiation field ($F = 10^7 \text{ erg s}^{-1} \text{ cm}^{-2}$), about a dozen of soft photons are absorbed within a cooling time and the temperature distribution function becomes very narrow around 2000 K and sublimation is likely. For hard photons ($h\nu \geq 50 \text{ eV}$), the PAH undergoes, independent of the strength of the radiation field, extreme temperature excursions. This indicates that PAH become photo-unstable either by absorption of a single hard photon, or by soft photons if there are many of them.

4. PAH destruction

The abundance of PAHs is determined by the competition between formation and destruction processes under the specific environmental conditions. Underlying processes are discussed, for example, by Omont (1986), Voit (1992), or recently by Micelotta et al. (2009a). Here we only consider PAH destruction by photons and generally assume that PAH formation is negligible. After photon absorption, a highly vibrationally excited PAH may relax through emission of IR photons or, if sufficiently excited, lose atoms. The latter process is called unimolecular dissociation and is discussed for interstellar PAHs by Allamandola (1989), Leger et al. (1989), Le Page et al. (2003), Rapacioli et al. (2006), and Micelotta et al. (2009b). Laboratory studies of PAH dissociation which can be applied to astrophysical situations are rare (Jochims et al. 1994). The photo-chemistry of PAHs is reviewed by Tielens (2005, 2008).

4.1. Procedure

In the disks of T Tau stars, the PAH abundance depends obviously on place and on time as the disk evolves. There is no general solution to the problem and to extract numbers, we have to radically simplify it. We wish to find some estimate of the location where PAHs become stable against photo-destruction. To derive a procedure, we recall that although after absorption of an energetic photon its energy is immediately distributed over all available vibrational modes (Allamandola et al., 1989), the excitation of a particular atom fluctuates and occasionally it is pushed into the continuum and leaves

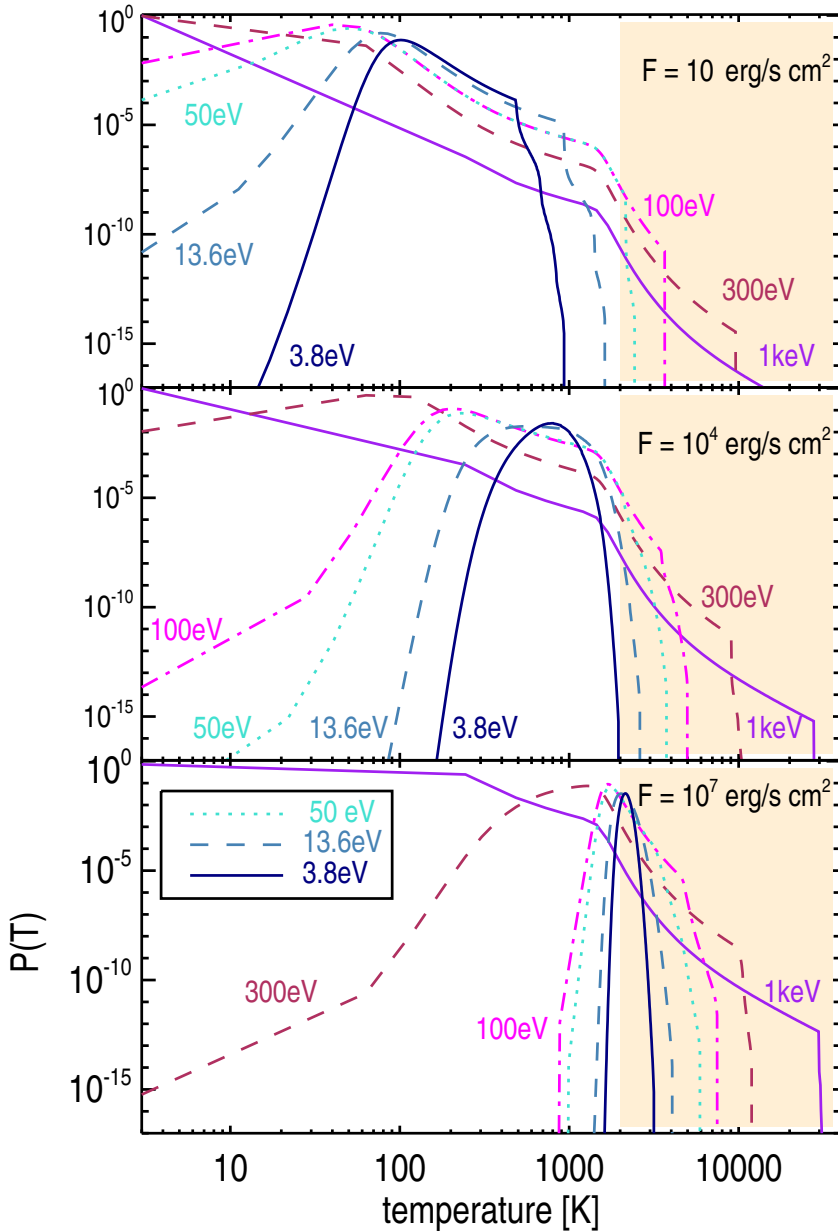


Fig. 3. The temperature distribution $P(T)$ of a PAH with 100 C atoms exposed to mono-chromatic radiation with $h\nu = 3.8, 13.6, 50, 100, 300$ eV and 1 keV. This set includes the mean photon energies of the four radiation components of the T Tauri star. The fluxes range from (top to bottom) $F = 10$ to 10^7 erg s $^{-1}$ cm $^{-2}$. Shaded area marks temperatures above the sublimation temperature of graphite.

the PAH. Quantitatively, the unimolecular dissociation can be written in Arrhenius form. In a classical description, an atom of critical (Arrhenius) energy E_0 detaches from a PAH of peak temperature T_p if the dissociation time

$$t_{\text{dis}} \sim \nu_0^{-1} e^{E_0/kT_p} \quad (7)$$

is shorter than the cooling time t_{cool} . A characteristic value for the vibrational frequency is $\nu_0 \sim 10^{13}$ s $^{-1}$. The “atom”, which may besides H or C

also be an atomic group like C_2H_2 , needs the time t_{dis} to overcome the critical internal barrier, E_0 , which is similar but not identical to the chemical binding energy. Micelotta et al. (2009b) quote E_0 of 3.2 eV for H-loss, 4.2 eV for C_2H_2 , 7.5 eV for pure C loss and 9.5 eV for C_2 . For the ISM they find $E_0 = 4.6$ eV and a somewhat larger value for PDR. The inverse of the dissociation time is the probability that a certain atom leaves the PAH per unit time.

The exponential term e^{E_0/kT_p} in Eq.(7) increases very rapidly as T falls and meaningful values (i.e. not too large ones) of t_{dis} are obtained only if $T_p > 1500$ K. Atoms will only detach when $t_{\text{dis}} < t_{\text{cool}}$. As the cooling time at these temperatures is for astrophysical applications of order 1 s, independent of the PAH size, the dissociation criterion reads

$$t_{\text{dis}} \lesssim 1 \text{ s} \quad (8)$$

It leads to a minimum temperature for destruction

$$T_{\text{dis}} = \frac{E_0}{k \ln \nu_0} \quad (9)$$

Assuming $E_0 \sim 5 \text{ eV}$, one gets $T_{\text{dis}} \simeq 2000 \text{ K}$. **At this high temperature, the internal energy of a PAH is reasonably well approximated by $3N_c k T_{\text{dis}}$ when also taking the presence of H-modes into account.** The minimum temperature T_{dis} is related to a minimum energy input ΔE . The PAH is therefore unstable to photons with

$$\Delta E \geq h\nu_c = 3N_c k T_{\text{dis}} = \frac{3}{\ln \nu_0} N_c E_0 \simeq 0.1 N_c E_0 \quad (10)$$

or when the number of carbon atoms

$$N_c \leq \frac{2\Delta E}{[\text{eV}]} \quad (11)$$

Micelotta et al. (2009b) find that a PAH with $N_c = 50$ requires an internal energy of about $\Delta E = 24 \text{ eV}$ to dissociate, which agrees with the above estimate (Eq. 11).

The minimum energy input required for dissociation can either be delivered by absorption of *i*) many soft photons, with a total energy $E_{\text{abs}} \geq \Delta E$ (Eq. 3), or *ii*) by a single hard photon, with energy $h\nu \geq \Delta E$. If a photon heats the PAH to a peak temperature much above T_{dis} , more than one atom will detach. The first expulsion occurs momentarily ($t_{\text{dis}} \ll 1 \text{ s}$). It consumes the energy E_0 plus some kinetic energy E_{kin} for the liberated atom. The new PAH temperature follows from

$$h\nu - E_0 - E_{\text{kin}} = 3(N_c - 1)kT \quad (12)$$

This happens x times until T has dropped to T_{dis} ,

$$h\nu - x(E_0 + E_{\text{kin}}) = 3(N_c - x)kT_{\text{dis}} \quad (13)$$

With $E_{\text{kin}} \sim 0.5 \text{ eV}$, we estimate that the total number of freed atoms is

$$x = \frac{h\nu - 3N_c k T_{\text{dis}}}{E_0 + E_{\text{kin}} - 3kT_{\text{dis}}} \simeq \frac{h\nu}{5 [\text{eV}]} - \frac{N_c}{10} \quad (14)$$

For $N_c = 100$, an average EUV photon ejects nine atoms and an X-ray photon destroys the whole PAH (column (5) in Table 2).

4.2. Disruption by Coulomb forces

For completeness, we also mention disruption of PAHs by Coulomb forces. Double or multiple ionization of a PAH loosens the binding of the peripheral H atoms as well as of the skeleton of carbon atoms. The ejection of K-shell electrons by X-ray photons ($h\nu > 284 \text{ eV}$) in combination with Auger electrons will amplify the process. Coulomb explosion is relevant mainly for small PAHs and neglected here.

5. Conditions for PAH survival

According to Eq. (10), PAHs are destroyed if the source emits photons of energy $h\nu \geq 0.1 N_c E_0$, irrespective of the distance to the star or its luminosity. For $N_c = 100$, the critical photon energy is only 50 eV (Eq.10). As T Tauri stars (or their jets) also radiate at X-rays and in the EUV, the surface of the disk should be devoid of PAHs unless *a*) the period over which hard photons are emitted is too short to destroy all PAHs; *b*) the PAHs are by vertical motions removed from the hard radiation before they are destroyed and there is an influx of PAHs from below; *c*) PAH destruction is compensated by PAH formation in the surface layer. The last effect should, in a hard photon environment where PAHs and carbon atoms are ionized, be prohibited by Coulomb repulsion (Voit, 1992).

5.1. Destruction time

The above PAH survival condition under *a*) can easily be dismissed. To estimate the time for PAH removal, t_{rem} , by the radiation component *i*, we note that most of the radiation is absorbed on the disk surface in a sheet of vertical optical depth τ_{\perp} equal to the grazing angle α_g of the incident light. We call this sheet the *extinction layer* (of radiation component *i*) and denote its geometrical thickness ℓ_i (see Fig.5). To first order, the PAHs in the extinction layer receive the stellar flux of Eq.(1) with $\tau_{\nu} = 1$. If the instability criterion of Eq.(10) is fulfilled, t_{rem} follows from $x N_{\gamma} t_{\text{rem}} = N_c$, where x is from Eq.(14), therefore

$$t_{\text{rem}} = \frac{N_c}{x} t_{\text{abs}} \quad (15)$$

With t_{abs} from Table 2, one sees that even at 100 AU, t_{rem} is short compared to the duration of the T Tauri phase ($\sim 10^6 \text{ yr}$, Bertout et al. 2007, Cieza et al. 2007).

5.2. Exposure time and vertical mixing

Next we consider the possibility that vertical motions in the disk lead to a continuous exchange between matter in the extinction layers, where almost all photons are absorbed and PAHs destroyed, and

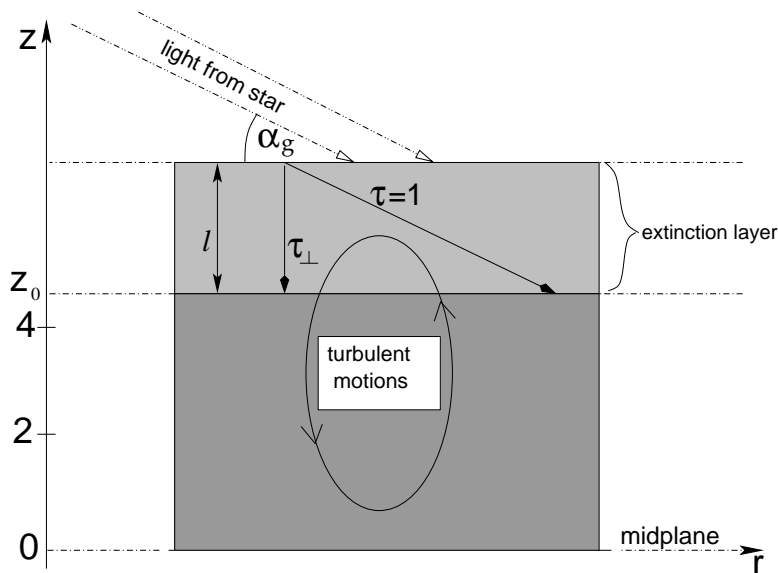


Fig. 5. Of each radiation component, $\sim 90\%$ is absorbed in what we call the extinction layer. The optical depth from its bottom to the star is one and in vertical direction equal to the grazing angle α_g . The height of its lower boundary, z_0 , declines with radius, but its geometrical thickness is rather constant ($\ell \sim 0.5 H$, see Fig.6). Vertical motions may replenish PAHs from below.

the layers below where PAHs are shielded and damaged ones possibly rebuilt (Fig.5). We assume that gas and dust are perfectly mixed in a mass ratio 130:1.

In a Keplerian disk that is isothermal in z -direction and in hydrostatic equilibrium, the gas density changes like

$$\rho(z) = \sqrt{\frac{2}{\pi}} \frac{\Sigma}{H} e^{-z^2/2H^2} \quad (16)$$

Here $\Sigma(r)$ is the surface density at radius r which is assumed to follow a power law,

$$\Sigma(r) = \int_0^\infty \rho(z) dz = \Sigma_0 \left[\frac{r}{\text{AU}} \right]^{-\gamma} \quad (17)$$

and

$$H(r) = \sqrt{kTr^3/GM_*m} \quad (18)$$

is the scale height, $M_* \simeq 1 M_\odot$ the stellar mass and m the mass of a gas molecule. For the surface density, reasonable numbers are $\gamma = 1$ and $\Sigma = 200 \text{ g cm}^{-2}$ (Hartmann et al. 1998, Kitamura et al. 2002, Dullemond et al. 2002, Rafikov & Colle 2006, Gorti & Hollenbach 2008), although the various estimates show considerable scatter.

For the radial variation of the gas temperature in the opaque mid plane, $T(r)$, we also adopt a power law,

$$T(r) = T_0 \left[\frac{r}{\text{AU}} \right]^{-\beta} \quad (19)$$

The mid plane is roughly isothermal in z because the optical depth is high and the net flux zero. It is much colder than the extinction layers because it is not exposed to direct stellar heating. The radiative transfer in the disk, including the energy equation, can be solved to any desired accuracy even when the disk is very opaque (see section 11.3.2 of Krügel 2006). As long as the dust in the mid plane is optically thick to its own emission, the results for $T(r)$ can be well approximated by putting in Eq.(19) $\beta = 0.5$ and $T_0 \sim 130 \text{ K}$ (as also suggested by Dullemond et al. 2007b or Chiang & Goldreich 1997).

Each extinction layer extends vertically from some value z_0 upwards to infinity (Fig.5). We give it a finite thickness ℓ by demanding that, say, 90% of the photons are absorbed between z_0 and $z_0 + \ell$. If v_\perp denotes the typical vertical velocity, for example, as a result of turbulence, PAHs are exposed to radiation for a time

$$t_{\text{exp}} = \frac{\ell}{v_\perp} \quad (20)$$

This is also the mean residence time of a PAH in the extinction layer. For PAHs to survive, t_{exp} must be smaller than t_{rem} Eq.(15). The height z_0 follows from

$$K \int_{z_0}^\infty \rho(z) dz = \alpha_g \quad (21)$$

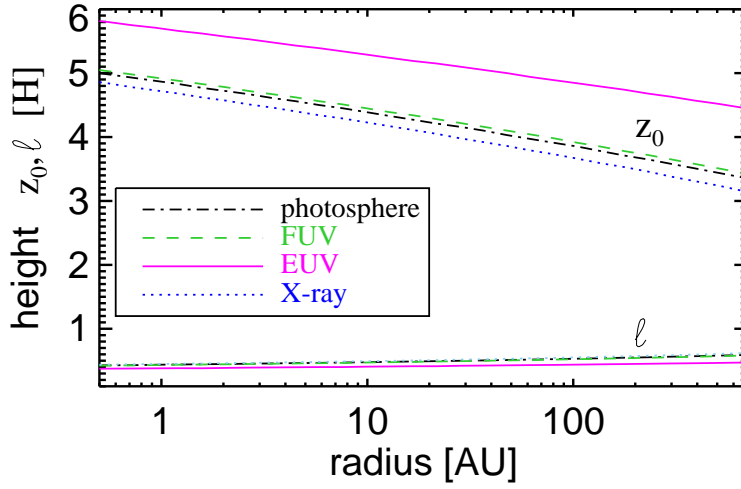


Fig. 6. The height, z_0 , of the bottom of the extinction layer and its thickness ℓ for the four radiation components (see Fig.5 and Eq.(21), (22)) for a grazing angle $\alpha_g = 3^\circ$. Due to the high gas densities, the EUV extinction layer is practically coincident with the ionization front and lies above the extinction layer of the other components. This implies that EUV radiation is absorbed first whereas the other components penetrate deeper. Neglecting ionization by the FUV component, the gas below the z_0 -line of the EUV radiation (top) is neutral.

and ℓ may be estimated from the condition that only 10% of the flux is absorbed above $z_0 + \ell$,

$$K \int_{z_0+\ell}^{\infty} \rho(z) dz = 0.1 \alpha_g \quad (22)$$

K is the mass absorption coefficient of gas and dust at the characteristic frequency of the particular radiation component (see Table 2). Because $\rho(z)$ changes rapidly, z_0 is rather insensitive both to α_g as well as K . For $\alpha_g/K = 10^{-8} \dots 10^{-2}$, one obtains $z_0 = 2.6H \dots 5.7H$. So in the V band, where absorption is only by dust ($K \simeq 200 \text{ cm}^2 \text{ g}^{-1}$) and for a grazing angle $\alpha_g = 3^\circ$, one gets $z_0 \simeq (4 \dots 5)H$ and $f_\ell = \ell/H \simeq 0.5$. The height z_0 where an extinction layer begins and its thickness are shown in Fig.6; ℓ is for all radiation components very similar ($\ell_i \sim H/2$, $i = 1, \dots, 4$). EUV photons are absorbed highest up, their extinction layer lies about one scale height above the others. X-rays penetrate slightly deeper than photospheric or FUV photons.

From Eq.(4), (15) and (20), one finds that vertical motions safeguard PAHs against destruction if

$$v_\perp > v_{\text{cr}} = \frac{\ell x}{t_{\text{abs}} N_c} = \frac{f_\ell H x}{4\pi r^2} \int_{\nu_c}^{\infty} \frac{L_\nu e^{-\tau_\nu} \kappa_\nu}{h\nu} d\nu \quad (23)$$

with ν_c from Eq.(10). When the scale height H is given by Eq.(18), $v_{\text{cr}} \propto r^{-(\beta+1)/2} = r^{-3/4}$. The values of v_{cr} , at a distance of 10 AU, are listed in Table 2 together with other quantities relevant to PAH survival.

One expects the disk also to be turbulent. Turbulence may be driven by various processes such as shear flows in the disk (Lin & Bodenheimer 1982), magneto-rotational instabilities (Balbus & Harley 1991) or velocity discontinuities at places where infalling matter (Cassen & Mossman 1981) or outflows (Elmegreen 1978) strike the disk surface. Until now it is not clear which type of turbulence dominates. We assume that for the size of the largest Eddies, ℓ_{ed} , the average turbulent velocity, v_t , grows linearly with the sound speed c_s . Various hydrodynamical 3-dimensional calculations (Cabot 1996, Boss 2004, Johansen & Klahr 2005, Fromang & Papaloizou 2006) support this view. The favoured parametrisation is $v_t = \alpha^q c_s$ with $q = 0.5$. This choice has consequences on the Eddy scale $\ell_{\text{ed}} = \alpha^{1-q} H$ and the turn over time $t_{\text{ed}} = \ell_{\text{ed}}/v_t = \alpha^{1-2q}/\Omega_K$, with Kepler frequency $\Omega_K = \sqrt{GM_*/R^3}$ (e.g. Dullemond & Dominik 2004). Weidenschilling & Cuzzi (1993) use $q = 1$ so that the Eddy scale is about the pressure scale height, $\ell_{\text{ed}} = H$, and larger than the thickness of the extinction layer, $\ell_{\text{ed}} > \ell \sim H/2$. Estimated values for α are in the range from 0.0001 up to 0.1 (Dullemond & Dominik 2004, Schr apler & Henning 2004, Youdin & Lithwick 2007). Taking $\alpha = 0.01$ the Eddy scale is 10 times smaller for $q = 0.5$ than for $q = 1$, and in addition larger turbulent velocities are obtained with $v_t = \sqrt{\alpha} c_s$, supporting a faster transport of the PAH. Identifying v_\perp in Eq.(23) with the turbulent velocity v_t and assuming a temperature dependence as in Eq.(19), we plot in Fig.7 the vertical velocity v_\perp as a function

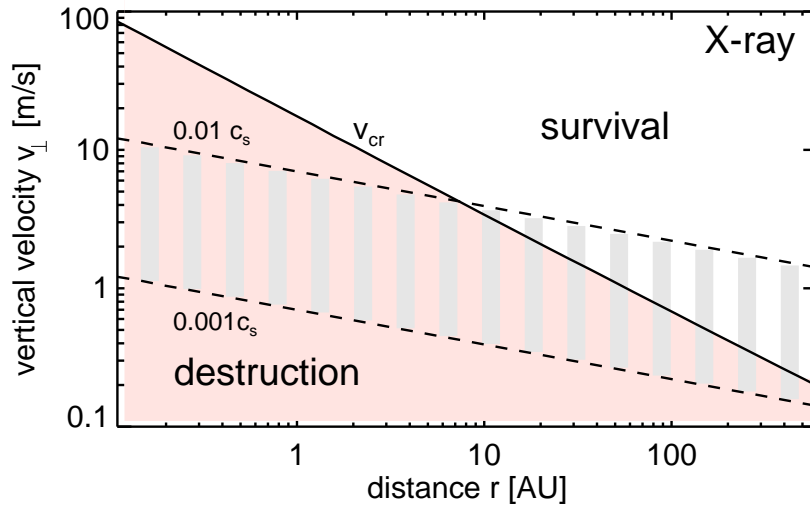


Fig. 7. The critical vertical velocity for PAH survival v_{cr} after Eq. (23) with respect to X-rays as a function of distance (full line). We identify the vertical velocity v_{\perp} with the turbulent velocity v_t . PAHs survive when $v_{\perp} = v_t > v_{\text{cr}}$, else they are destroyed (shaded areas) by expulsion of atoms. The hatched strip between the dashed lines shows the range where v_{\perp} is between $0.001 c_s$ and $0.01 c_s$ (where c_s is the sound velocity).

Table 2. Quantities relevant to PAH survival.

	(1)	(2)	(3)	(4)	(5)	(6)	(7)	(8)	(9)
component	$h\bar{\nu}$ eV	κ 10^{-4}Å^2	η	K/K_V	x	z_0/H	ℓ/H	t_{abs}	v_{cr} m/s
photosphere	2.7	700	$\ll 1$	1.2	-	4.4	0.5	5 s	-
FUV	4.2	700	$\ll 1$	1.5	-	4.5	0.5	120 s	-
EUV	97	36	~ 0.5	110	9	5.3	0.4	9 days	2900
X-ray	1100	0.17	$\ll 1$	0.55	100	4.2	0.5	290 yr	3.4

- (1) The mean energy of destructive photons, $h\bar{\nu}$, from Eq.(5) at the bottom of the extinction layer (see Fig.5); for photospheric and FUV photons we put $\nu_c = 0$ and for EUV and X-rays we integrate for $\nu \geq \nu_c$ (Eq. 10);
(2) absorption cross section, κ , per C atom at frequency $\bar{\nu}$;
(3) approximate mean degree of ionization of the gas in the extinction layer;
(4) extinction cross section of gas and dust at frequency $\bar{\nu}$ normalized to $K_V = 200 \text{ cm}^2 \text{ g}^{-1}$;
(5) number of expelled atoms, x , per absorption event from Eq.(14);
(6) altitude of the bottom of the extinction layer in units of the scale height H ;
(7) thickness of extinction layer;
(8) mean time t_{abs} from Eq.(4) in which one photon is absorbed;
(9) critical vertical velocity for PAH survival.
Note: $z_0, \ell, t_{\text{abs}}$ and v_{cr} refer to $r = 10 \text{ AU}$.

of radius. The figure also shows the critical velocity for PAH survival, v_{cr} , with respect to X-rays. Note that the critical velocity is for the X-ray radiation component insensitive to the particular choice of E_0 and ν_c (Eq. 10, 23). When $v_{\perp} = 0.01 c_s$, PAHs can survive at distances $r > 10 \text{ AU}$; when v_{\perp} is considerably smaller than $0.01 c_s$, they cannot.

Critical velocities for PAH survival are much higher for EUV than for X-ray photons (Table 2). EUV radiation will therefore always destroy PAHs but, as depicted in Fig.6, the EUV extinction layer

is the topmost and below it, PAHs may survive and be excited.

If PAHs are removed from the extinction layer before they are destroyed, they must, in order to be detected, at the same rate be injected from below. Therefore, the critical velocity can alternatively be expressed through

$$\frac{1}{t_{\text{rem}}} \int_{z_0}^{z_0+\ell} \rho(z) dz \simeq \rho(z_0) v_{\text{cr}} \quad (24)$$

which leads to similar values. We note that the mass reservoir below the extinction layer is sufficient to

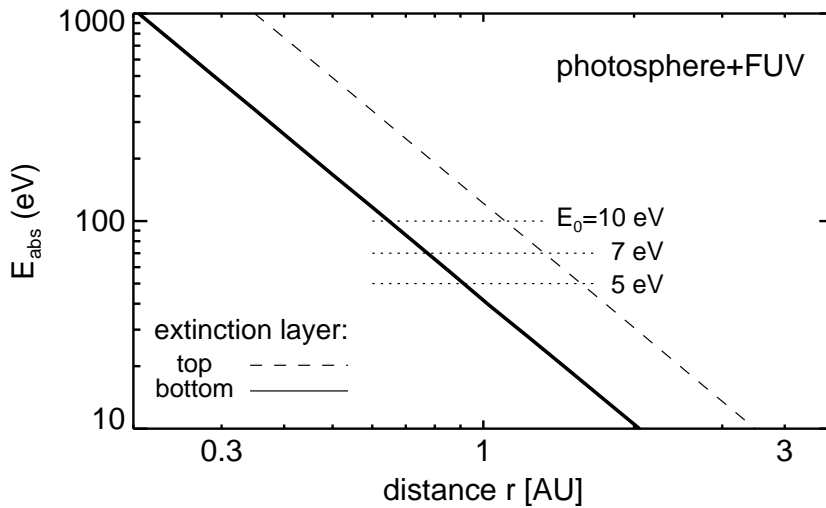


Fig. 8. The energy E_{abs} (Eq.3), which is absorbed by a PAH of $N_c = 100$ carbon atoms, as a function of distance from the star. The PAH is exposed to the photospheric and FUV radiation component described in Table 1. The dashed line refers to the top of the extinction layer ($\tau = 0$) and the full line to its bottom ($\tau = 1$). For Arrhenius energy of $E_0 = 5, 7$ and 10 eV, the minimum energy input ΔE (Eq.10) for PAH dissociation is indicated by the dotted lines.

sustain, over the lifetime of the disk t_{life} , the required mass influx ρv_{cr} .

5.3. PAH dissociation by soft versus hard photons

The energy E_{abs} (Eq.3), which is absorbed by a PAH of $N_c = 100$ carbon atoms, is shown in Fig. 8 as a function of distance from the star. The PAH is exposed to the photospheric and FUV radiation component described in Table 1 and results are shown for the top ($\tau = 0$) and the bottom ($\tau = 1$) of the extinction layer. The minimum energy input ΔE (Eq.10) for PAH dissociation depends on the choice of the Arrhenius energy E_0 and is indicated for $E_0 = 5, 7$ and 10 eV, respectively. In this picture, for $E_0 = 5$ eV and at the bottom of the extinction layer, PAHs are dissociated by soft photons up to 1 AU. For X-rays, however, we find that PAH destruction occurs typically at distances up to ~ 10 AU or even larger (Fig.7). Dissociation of PAH acts for soft (photospheric and FUV) photons on much shorter distances than for hard photons (X-ray component).

6. Large grains

Observations of T Tauri stars at millimeter wavelengths (Testi et al. 2003, Lommen et al. 2007) and in the mid infrared (van Boekel et al. 2003, Przygodda et al., 2003, Kessler-Silacci et al. 2006, Bouwman et al. 2008, Watson et al. 2009) suggest that grains in T Tauri disks are at least 10 times larger than those in the ISM. As such large grains

may also be present in the top disk layer we estimate how this would affect the stability analysis of PAHs. We first note that in case of homogeneous mixing an increase in particle size would not alter the dust-to-gas mass ratio.

Should the grains be much larger than the wavelength, the absorption coefficient per gram of dust, $K_{\text{d},\lambda}$, would decrease roughly like one over grain radius whereas the ratio $K_{\text{d},\lambda}/K_{\text{d},\nu}$ would still roughly be given by the values in Table 2. For hard X-rays, on the other hand, $K_{\text{d},\lambda}$ is not sensitive to grain size.

Therefore, if disk grains are on average ten times bigger and thus 10^3 more massive than interstellar ones, we expect that the height z_0 to which the stellar radiation components can penetrate (see Fig.6) stays the same for X-rays, but also for EUV radiation because EUV absorption is due to gas, not dust. However, optical and FUV photons will reach farther down, about half a scale height, so that there may be a thin disk layer ($\sim H/4$) where PAHs are shielded from X-rays and EUV photo-dissociation and excited by optical or FUV radiation.

7. Conclusion

In the search for an explanation why most T Tauri stars do not exhibit PAH features and only a few do, we investigate which processes can remove PAHs from the surface layer of T Tauri disks and under which conditions they should be present. Clearing of PAH through interaction with planets seems not

an efficient process (Geers et al 2007b) and we show that PAH under-abundance can be caused by radiative destruction. We use a fiducial model for the photon emission of the T Tauri star that includes, beside the photosphere, FUV and EUV radiation and an X-ray component.

1. We introduce for each stellar radiation component the notion of *extinction layer* as the place where $\sim 90\%$ of the photons are absorbed. EUV photons are mainly absorbed by gas, X-rays by gas and dust alike and the photospheric and FUV component are only attenuated by dust. The extinction layer of all four components have a similar geometrical thickness and their bottom is at similar elevation z_0 , except for the EUV extinction layer which lies higher up (Fig.6).
2. PAH may be radiatively destroyed, by unimolecular dissociation, where one or several atoms are expelled after photon absorption.
3. Destruction by the photospheric and FUV radiation component (soft photons), increases with the strength of the radiation field and is very efficient below 1 AU.
4. Hard photons can dissociate PAHs at all distances and their efficiency grows with the hardness of the photons. Without some counter process, all PAHs (in layers where they can be excited) would be destroyed within a time short compared to the lifetime of the disk.
5. Although grains in the disk surface are presumably larger than interstellar ones, the stability analysis of PAHs would not change significantly.
6. Therefore, in disks where PAHs are detected, there must be some survival channel. Because creation of PAHs in the extinction layer is too slow to compete with PAH destruction (Voit 1992), we suggest *vertical mixing* as a result of turbulence. It can replenish PAHs or remove them from the reach of hard photons.
7. For standard disk models, the minimum velocity for PAH survival is proportional to $r^{-3/4}$ and equals ~ 5 m/s at 10 AU. If turbulent velocities are proportional to the sound speed a velocity $v_t \geq 5$ m/s would imply $v_t/c_s \gtrsim 0.01$ as PAH survival condition. Theoretical predictions for this ratio have a large spread but in accordance with the observational fact that PAH features are usually absent it seems that generally the condition is not fulfilled.
8. A higher PAH detection rate is found in Herbig Ae/Be stars. In our picture this is explained as their destructive hard radiation component is relatively weak ($L_x/L_* \lesssim 10^{-7}$, Preibisch et al. 2006) and because the intensity of the PAH emission from large distance from the star is larger given their higher optical luminosities.

Acknowledgements. We thank the second anonymous referee for constructive comments.

References

- Akeson R.L., Walker C. H., Wood K., et al., 2005, ApJ 622, 440
- Allamandola L.J., Tielens A.G.G.M., Barker J.R., 1989, ApJS 71, 733
- Acke B., & van den Ancker, 2004, A&A 426, 151
- Balbus S.A., Hawley J.F., 1991, ApJ 376, 214
- Boss A.P., 2004, ApJ 610, 456
- Brown J.M., Blake G.A., Qt C., Dullemond C.P., Wilner D.J., 2008, ApJ, L109
- Balucinska-Church M., & McCommon D., 1992, ApJ 400, 699
- Bertout C., Siess L., Cabrit S., 2007, A&A 473, L21
- Bouwman J., Henning Th., Hillenbrand L.A., 2008, ApJ 683, 479
- Cabot W., 1996, ApJ 465, 874
- Calvet N., Gullbring E., 1998, ApJ 509, 802
- Cassen P.M., Mossman A., 1981, Icarus 48, 353
- Chiang E.I., Goldreich P., 1997, ApJ 490, 368
- Cieza L., Padgett D.L., Stapelfeldt K.R., et al., 2007, ApJ 667, 328
- CRC Handbook of Chemistry & Physics, 2005, Taylor & Francis, p.6ff
- Dullemond C.P., van Zadelhoff G.J., Natta A., 2002, A&A 389, 464
- Dullemond C.P., Dominik C., 2004, A&A 421, 1075
- Dullemond C. P., Henning Th., Visser R., et al., 2007, A&A 473, 457
- Dullemond C. P., Hollenbach D., Kamp I., D'Alessio P., 2007b, in: Protostars and Planets V, B. Reipurth, D. Jewitt, and K. Keil (eds.), University of Arizona Press, Tucson, p.555
- Dwek E., & Smith R.K., 1996, ApJ 459, 686
- Elmegreen B.G., 1978, Moon and Planets 19, 21
- Evans N.J., Allen L.E., Blake G.A., et al., 2003, PASP 115, 965
- Fromang S., Papaloizou J., 2006, A&A 452, 751
- Furlan E., Hartmann L., Calvet N., et al., 2006, ApJS 156, 568
- Geers V.C., Augereau J.-C., Pontoppidan K. M., et al., 2006, A&A 459, 545
- Geers V.C., van Dishoeck E.F., Pontoppidan K.M., et al., 2007a, A&A 476, 279
- Geers V.C., Pontoppidan K.M., van Dishoeck E.F., et al., 2007b, A&A 469, L35
- Geers V.C., van Dishoeck E.F., Pontoppidan K.M., et al., 2009, A&A 495, 837
- Güdel M., Skinner, S. L., Mel'Nikov S. Yu., 2007, A&A 468, 353
- Guhathakurta P., Draine B.T., 1989, ApJ 345, 230
- Gorti U., Hollenbach D., 2008, ApJ 683, 287
- Kassis M., Adams J.D., Campbell M.F., 2006, ApJ 637, 823
- Kessler-Silacci J., Augereau J.-C., Dullemond C., et al., 2006, ApJ 639, 275
- Kitamura Y., Momose M., Yokogawa S., et al., 2002, ApJ, 581, 357
- Krügel E., 2006 *An introduction to the Physics of Interstellar Dust*, IoP, Sect. 5.4 and 10.2
- Johansen A., Klahr H., 2005, ApJ 634, 1353
- Judge P.G., Solomon S.C., Ayres T.R., 2003, ApJ 593, 534
- Leach S., Eland J.H.D., Price S.D., 1989a, J. Phys. Chem. 93, 7575
- Leach S., Eland J.H.D., Price S.D., 1989b, J. Phys. Chem. 93, 7583
- Leger A., D'Hendecourt L., Boissel P., Desert F.X., 1989, A&A 213, 351
- Le Page V., Snow T.P., Bierbaum V.M., 2003, ApJ 584, 316
- Lin D.N.C., Bodenheimer P., 1982, ApJ 262, 768
- Lommen D., Wright C.M., Maddison S.T., et al., 2007, A&A 462, 211

Meeus G., Waters L.B.F.M., Bouwman J., et al. 2001, A&A 365, 476
Micelotta E.R., Jones A.P. and Tielens A.G.G.M., 2009a, A&A in press
Micelotta E.R., Jones A.P. and Tielens A.G.G.M., 2009b, A&A in press
Morrison R., & McCommon D., 1983, ApJ 270, 119
Muzerolle J., Hartmann L. and Calvet N., 1998, AJ 116, 2965
Muzerolle J., Calvet N., Hartmann L., D'Alessio P., 2003, ApJ 597, L149
Omont A., 1986, A&A 166, 159
Peeters E., Hony S., van Kerckhoven C., et al., 2002, A&A 390, 1089
Preibisch T., Kim Y.-C., Favata F., et al., 2006, ApJSS 160, 401
Przygodda F., van Boekel R., Abraham, P., et al., 2003, A&A 412, 43
Rafikov R.R., de Colle, F., 2006, ApJ 646, 275
Rapacioli M., Calvo F., Joblin C., et al., 2006, A&A 460, 519
Ruhl E., Price S.D., Leach S., 1989, J. Phys.Chem. 93, 6312
Salpeter E.E., 1977, ARA&A 15, 267
Schräpler R., Henning Th., 2004, ApJ 614, 960
Schutte W. A., Tielens A. G. G. M. and Allamandola L. J., 1993, ApJ 415, 397
Siebenmorgen R., Prusti T., Natta A., Müller T.G., 2000, A&A 361, 258
Stahler S.W., Shu F.H., Taam R.E., 1980 ApJ 242, 226
Stelzer B., Micela G., Hamaguchi K., Schmitt J.H.M.M., 2006, A&A 457, 223
Stelzer B., Flaccomio E., Briggs K., 2007, A&A 468, 463
Sterzik M.F., Schmitt H.M.M., 1997, AJ 114 (4), 1673
Testi L., Natta A., Shepherd D.S., Wilner D.J., 2003, A&A 403, 323
Tielens A.G.G.M., 2005, The Physics and Chemistry of the Interstellar Medium, ISBN 0521826349, Cambridge University Press, Sect. 6.4
Tielens A.G.G.M., 2008, ARA&A 46, 289
Visser R., Geers V. C., Dullemond C. P., et al., 2007, A&A 466, 229
Voit G.M., 1992, MNRAS 258, 841
van Boekel R., Waters L.B.F.M., Dominik C., et al., 2003, A&A 400, 21
van Boekel R., Min M., Leinert C., et al., 2004, Nature 432, 479
Waelkens C., Waters L.B.F.M., de Graauw M.S., et al., 1996, A&A 315, L245
Watson D.M., Leisenring J.M., Furlan E., et al., 2009, ApJS 180, 84
Weidenschilling S.J., Cuzzi J.N., 1993, *Protostars and Planets III* (A93-42937 17-90), p. 1031-1060.
Youdin A.N., Lithwick Y., 2007, Icar 192, 588